



Contents lists available at ScienceDirect

Tectonophysics

journal homepage: www.elsevier.com/locate/tecto

Geophysical insights and early spreading history in the vicinity of the Jan Mayen Fracture Zone, Norwegian–Greenland Sea

Laurent Gernigon^{a,*}, Odleiv Olesen^a, Jörg Ebbing^a, Susann Wienecke^b, Carmen Gaina^a, John Olav Mogaard^a, Morten Sand^c, Reidun Myklebust^d

^a Geological Survey of Norway (NGU), Norway

^b Statoil Research Centre, Norway

^c Norwegian Petroleum Directorate, Norway

^d TGS-NOPEC Geophysical Company ASA, Norway

ARTICLE INFO

Article history:
Received 22 August 2007
Accepted 24 April 2008
Available online xxxx

Keywords:
Jan Mayen Fracture Zone
Volcanic margin
Breakup
Triple junction
Aeromagnetic
Oceanic crust

ABSTRACT

Using a new high-resolution aeromagnetic survey (JAS-05) that was acquired along the trend of the Jan Mayen Fracture Zone (JMFZ), west of the Vøring volcanic margin, we investigated the geodynamic framework of the early spreading evolution of the Norwegian–Greenland Sea. The tectonic structure, main faults and magnetic chrons have been reinterpreted based on new magnetic gridded data and integrated with bathymetry, gravity and seismic data. The new interpretation reveals more details about the early spreading history of the Norwegian–Greenland Sea in the vicinity of the JMFZ. Although anomalous melt production (seaward-dipping reflectors, underplating) associated with the breakup of the Mid-Norwegian margin has been described in many studies, we present data that suggest that significant magmatism continued episodically during the opening of the Norwegian–Greenland Sea along the trend of the JMFZ. The Vøring Spur (VS), an anomalous oceanic high, lying north of the eastern segment of the JMFZ exhibits a contrasting Bouguer gravity low and a complex magnetic signature. The gravity signature of the VS can be modelled and explained as an abnormal thick oceanic crust, which locally can reach up to 15 km. We propose that the thick oceanic crust (overcrusting) was syn-rift and formed during Mid- to Late Eocene. A plate reconstruction at Eocene time suggests that the VS could be part of a triple junction initiated during the breakup between the Vøring Marginal High and the Greenland part of the Traill–Vøring igneous complex, now located offshore East Greenland. Mantle upwelling beneath the early spreading ridge and/or local stress reorganisation could have induced transtension and lithospheric thinning along the JMFZ and magmatic activity would have increased locally along this ‘leaky transform’. We suggest that the Early Tertiary tectono-magmatic processes that operated in the Norwegian–Greenland Sea are similar to the processes involved in the modern triple junction evolution of the Azores Plateau region.

Crown Copyright © 2008 Published by Elsevier B.V. All rights reserved.

1. Introduction

The Norwegian–Greenland Sea comprises a complex system of active and aborted spreading ridges and oceanic basins, initiated in earliest Eocene times after the continental breakup between Eurasia and Greenland. In the central part of the Norwegian–Greenland Sea, the Jan Mayen Fracture Zone (JMFZ) forms broad and dominant scars on the sea-floor and represents a major crustal boundary of the Northeast Atlantic (Johnson and Eckhoff, 1966; Talwani and Eldholm, 1977) (Fig. 1).

This region has been the subject of many key geophysical surveys and plate kinematics investigations (Talwani and Eldholm, 1977;

Nunns, 1982; Sirastava and Tapscott, 1986). Compared with the Norwegian continental shelf, where intense petroleum exploration contributed substantially to our general knowledge of the volcanic margin formation and pre-breakup rift system (Skogseid et al., 1992; Eldholm and Grue, 1994; Ren et al., 1998; Brekke, 2000; Berndt et al., 2001a; Gernigon et al., 2003; Lien, 2005; Mjelde et al., 2007; Osmundsen and Ebbing, submitted for publication), the tectono-magmatic evolution of the Norwegian Sea oceanic domain remained underexplored and is far from being well-understood.

Detailed geophysical description of the rift to drift transition along the Norwegian–Greenland Sea is essential to better understand and evaluate rift dynamics, fundamental geodynamic processes and changes in paleogeography. The JMFZ area was covered by vintage surveys that were included in the magnetic compilation of Verhoef et al. (1997) (Fig. 2a). A few modern aeromagnetic surveys covering neighbouring areas have shown that a large part of the old data could be misinterpreted due to

* Corresponding author. Norges geologiske undersøkelse (NGU), Geological Survey of Norway, Continental Shelf Geophysics, Leiv Eirikssons vei 39, N-7491 Trondheim, Norway. Tel.: +47 73 90 44 37; fax: +47 73 92 16 20.

E-mail address: Laurent.Gernigon@ngu.no (L. Gernigon).

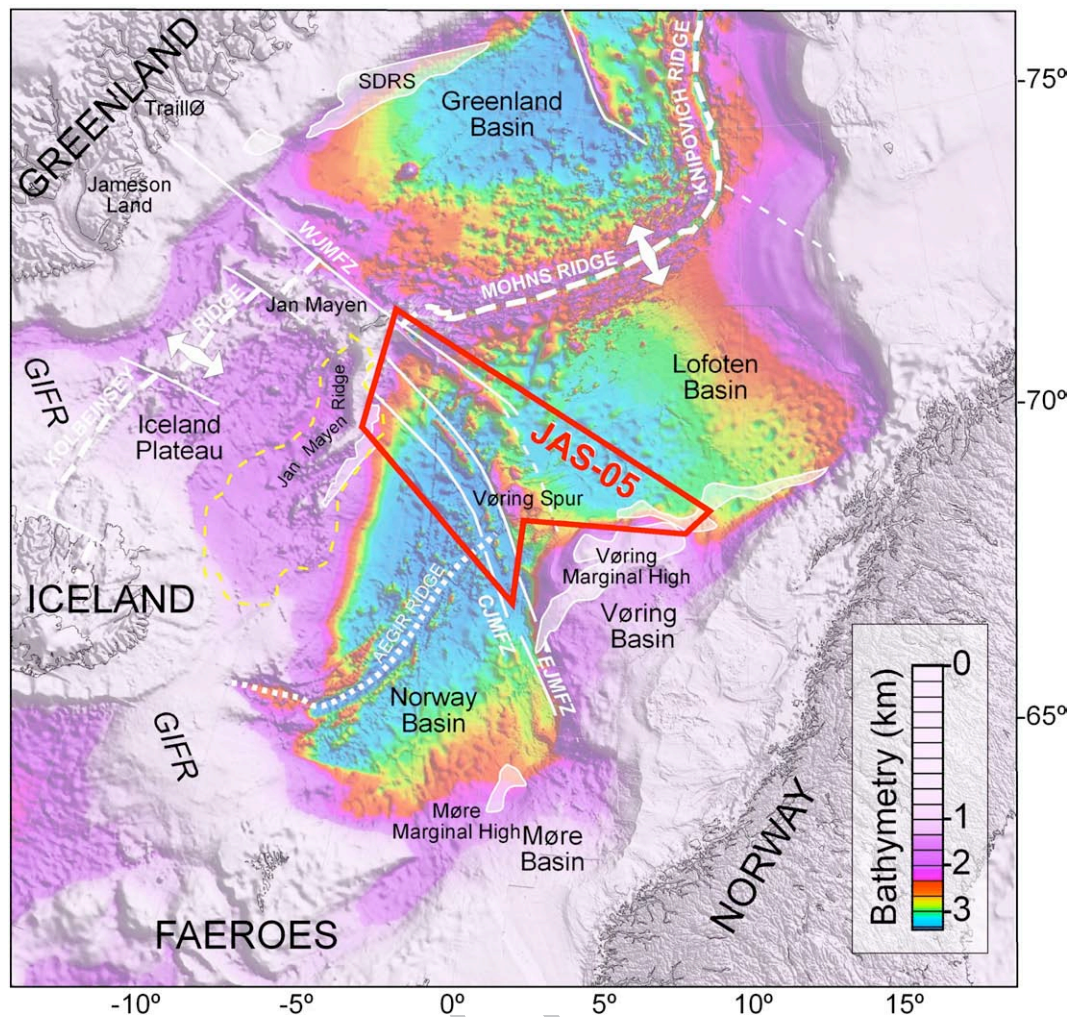


Fig. 1. Bathymetric map and main physiographic features of the Norwegian–Greenland Sea. Sea-floor spreading led to the formation of Reykjanes, Aegir and Mohns Ridges. Spreading along the Aegir Ridge decreased until ceasing in the Oligocene. A progressive ridge jump along the Kolbeinsey Ridge happened during the same period, connecting the Mohns and Kolbeinsey Ridges and leading to the formation of the Jan Mayen microcontinent. The Jan Mayen Fault Zone (JMFZ) consists of three distinct segments named the western (WJMFZ), eastern (EJMFZ) and central Jan Mayen Fractures zones (CJMFZ), respectively. The blue polygon represents the outline of the JAS-05 survey and main study area along the JMFZ. Seaward-dipping reflector sequences (SDRs) represent thick volcanic lava flows extruded during the breakup along the Vøring Marginal High (white outlines). GIFR: Greenland–Iceland–Faeroes Ridge.

geophysical artefacts, caused by inappropriate levelling, poor navigation records and/or inadequate and sparse spacing of old, pre-existing, magnetic profiles (Olesen et al., 2007).

On the basis of these ambiguous data, the spreading evolution of the Norwegian–Greenland Sea and JMFZ has been nonetheless the subject of many regional and geodynamic studies (Talwani and Eldholm, 1977; Hagevang et al., 1983; Skogseid and Eldholm, 1987; Blystad et al., 1995; Torsvik et al., 2001; Lundin and Doré, 2002; Mosar et al., 2002; Tsikalas et al., 2002; Scott et al., 2005; Olesen et al., 2007; Scheck-Wenderoth et al., 2007). Some contributions particularly raise challenging questions about the timing, variability and origin of atypical magmatic events affecting the Norwegian–Greenland Sea and its surrounding volcanic margins (Breivik et al., 2006; Greenhalgh and Kuszniir, 2007; Meyer et al., 2007; Olesen et al., 2007; Breivik et al., 2008). These contributions concur that a clear understanding of the tectonic and magmatic history of the Norwegian oceanic domain is essential when dealing with breakup, spreading rate evolution, intra-plate magmatism and the influence of deep but controversial sub-lithospheric mechanisms that may involve or not the Icelandic mantle plume. However, a proper understanding of the dynamics of breakup, evolution of basins situated on conjugate margins and the formation of the oceanic crust requires higher quality data. In terms of isostasy, flexure and the thermal evolution of deep offshore basins Gernigon et al. (2006), Lucazeau et al.

(2003) and Kuszniir and Karner (2007) have shown notably that the rift to drift evolution of any rifted margin should be considered for reliable basin modelling. Fundamentally, a better investigation of the spreading history and associated magmatic events should help us to better assess the parameters and mechanisms involved during and after the onset of the breakup on the Mid-Norwegian margin.

The main objective of this contribution is to update and re-examine the geophysical and tectonic setting of the Norwegian–Greenland Sea in the vicinity of the JMFZ, west of the Vøring Marginal High, an area that has been affected by significant breakup magmatism (Fig. 1). We present and discuss new regional aeromagnetic data (JAS-05) acquired along the trend of the JMFZ (Figs. 1, 2). This new aeromagnetic survey has been integrated with gravity and modern seismic data, in order to document important aspects of the early spreading and magmatic history of the Norwegian–Greenland Sea and in particular the structure and evolution of the JMFZ. We also focus on the structure and significance of the Vøring Spur (VS), an intriguing and atypical bathymetric high located along the trend of the JMFZ (Fig. 1). Lying along the trend of the JMFZ, the VS has been named in the Law of the Sea context (Symonds and Brekke, 2004) and very few contributions have attempted to interpret and understand this peculiar oceanic feature (Symonds and Brekke, 2004; Breivik et al., 2008). To conclude, we

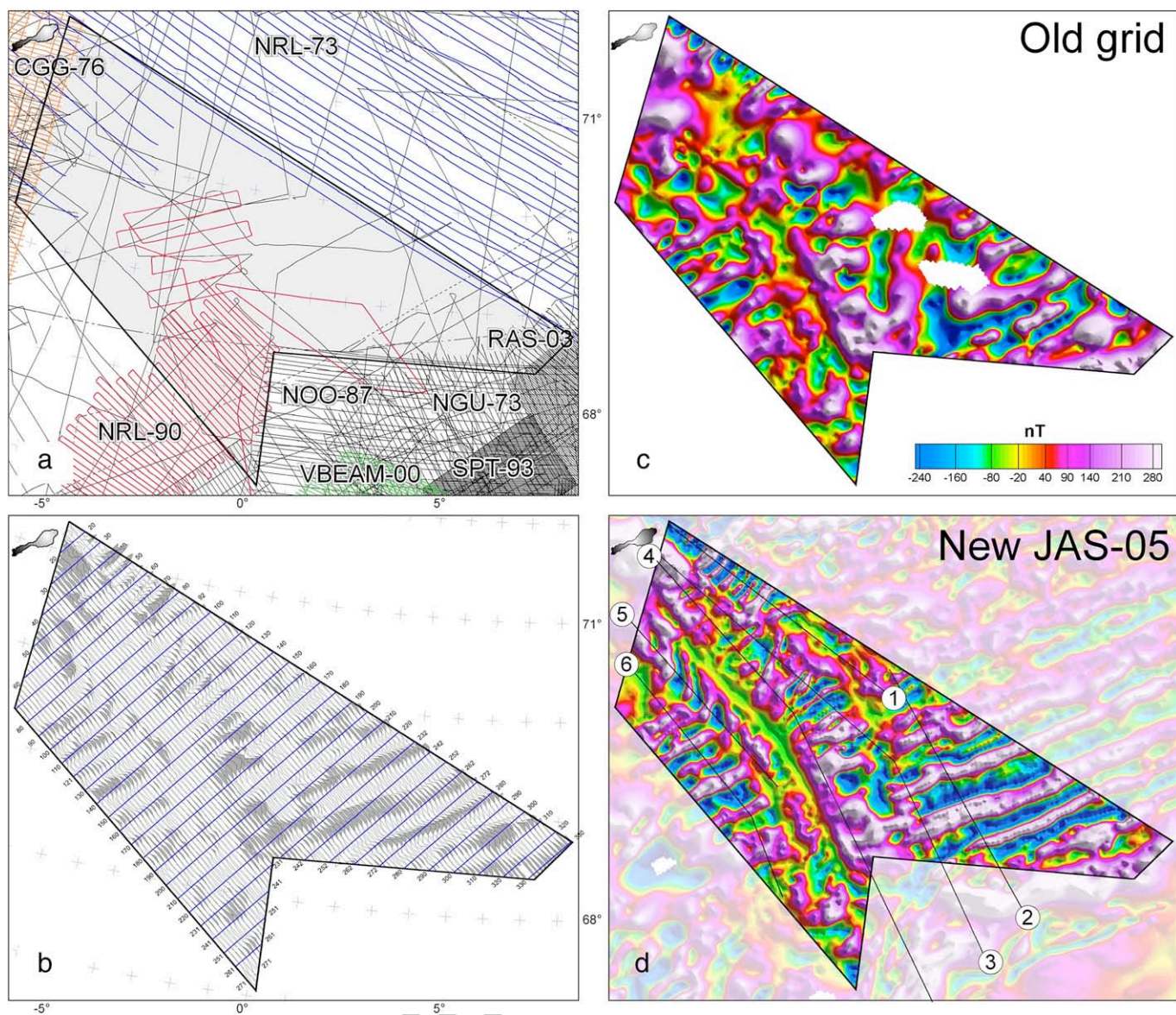


Fig. 2. a) Outline of the JAS-05 survey and tracks of older magnetic profiles. b) Magnetic anomaly profiles along the NW-SE profiles and distribution of the NE-SW tie profiles (in blue). c) Map of gridded anomalies (1×1 km) based on vintage profiles (e.g. Verhoef et al., 1997; Olesen et al., 2007). d) Comparison with the updated map of gridded anomalies (1×1 km) after full statistical levelling, IGRF correction and 1×1 km minimum curvature gridding of the JAS-05 profiles.

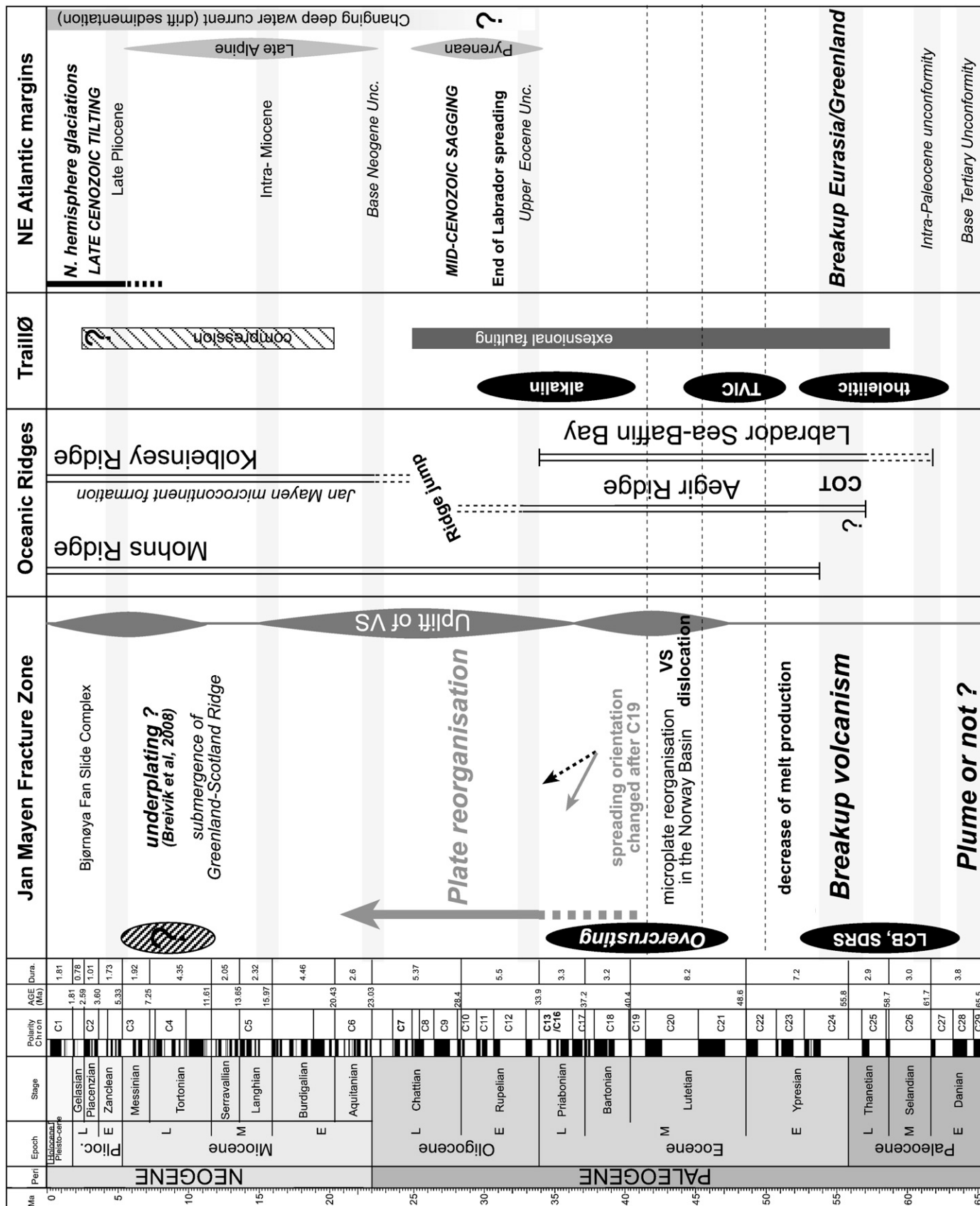
108 propose a new geodynamic scenario and implications of the early
109 spreading of the Norwegian-Greenland Sea.

110 2. Geodynamic and geological background

111 The Norwegian-Greenland Sea formed when Eurasia and Green-
112 land separated in Early Tertiary time (Figs. 1, 3). Final breakup geo-
113 metry is partially preserved by the present-day continent-ocean
114 boundary (COB) whose age was interpreted as pre-chron 24B (there-
115 fore older than 53.3 Ma according to the timescale of Cande and Kent
116 (1995) (Hagevang et al., 1983; Skogseid and Eldholm, 1987). This major
117 tectonic event was accompanied by significant volcanic activity associ-
118 ated with the formation of the North Atlantic Igneous Province
119 (Talwani and Eldholm, 1977; Skogseid and Eldholm, 1987; Eldholm and
120 Grue, 1994). Seaward-dipping reflectors sequences (SDRs), sill/dykes
121 intrusions, and high-velocity lower crustal bodies, commonly related
122 (or partly related) to underplated mafic or ultramafic intrusions, wit-
123 nessed the atypical but controversial melt production along the con-
124 jugate volcanic margins (Eldholm and Grue, 1994; Berndt et al., 2001a;

Breivik et al., 2006; Mjelde et al., 2007). It has been suggested that the
125 Iceland plume caused and/or influenced the breakup of continents and
126 voluminous breakup magmatism at the scale of the North Atlantic
127 (Eldholm and Grue, 1994). Although a mantle plume could explain the
128 formation of this regional magmatic event, some authors have argued
129 that the voluminous breakup magmatism is more complex and may
130 reflect compositional heterogeneities and/or plate-driven dynamic
131 processes in the upper mantle and not necessarily an excess mantle
132 temperature associated with a deep thermal boundary (Van Wijk et al.,
133 2001; Korenaga, 2004). Since none of the models explains all the
134 observations, some mixed or hybrid models have been also proposed
135 (Meyer et al., 2007).
136

137 After breakup, normal sea-floor spreading occurred simultaneously
138 along the Mohns and Aegir Ridges that are offset along the JMFZ, that
139 acted as a complex and active oceanic transform zone between the two
140 spreading systems (Talwani and Eldholm, 1977). After breakup, anom-
141 alous melt production decreased in the Norwegian-Greenland Sea.
142 South of this area, along the Greenland-Iceland-Faroes Ridge (Fig. 1), the
143 thick oceanic crust (17-35 km) indicates an anomalous and higher melt
144



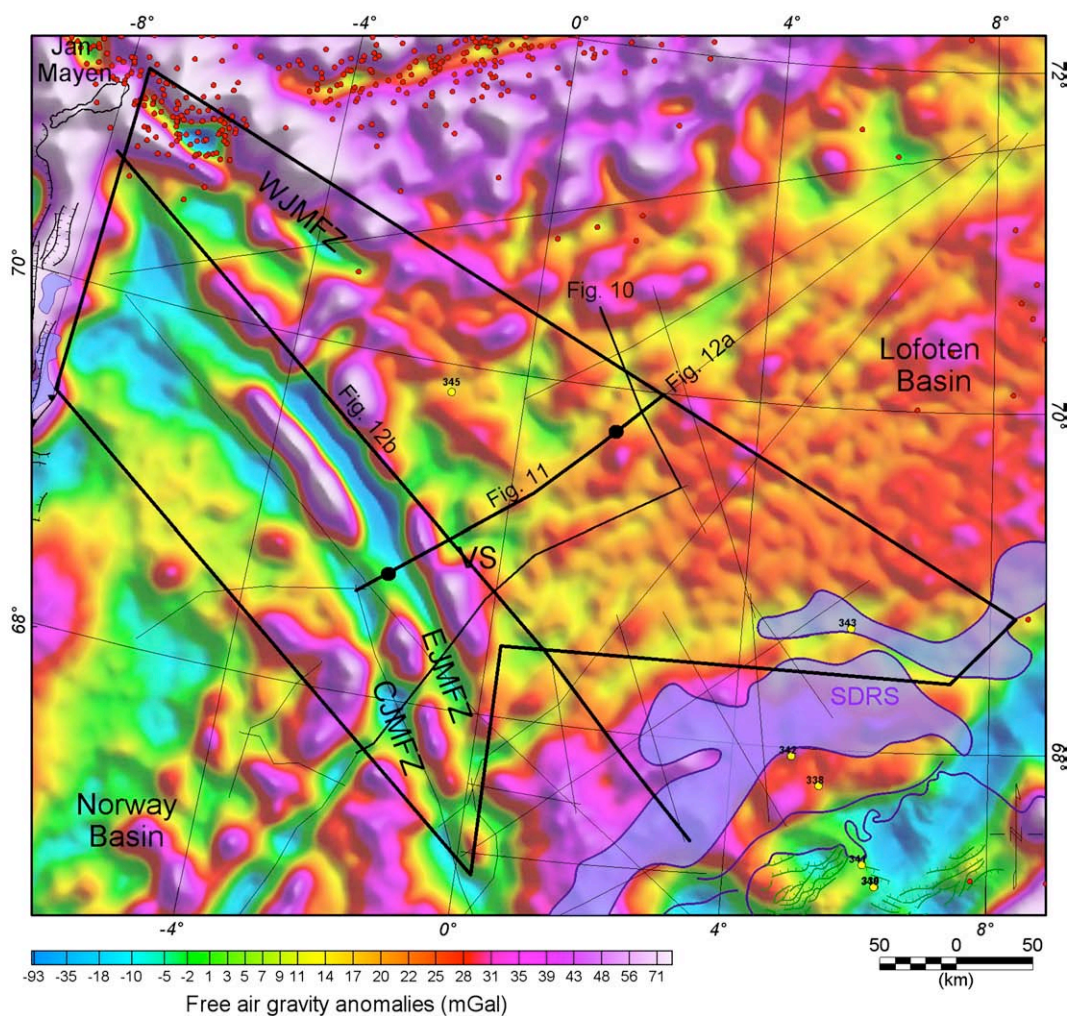


Fig. 4. Free-air gravity along the study area. The map also shows the seismic database available for the study. The red circles represent the earthquake distribution from the USGS National Earthquake Information Center (<http://earthquake.usgs.gov/regional/ncic/>). VS: Vøring Spur.

144 production due to the proximity of the Iceland hotspot (Smallwood et al.,
145 1999; Breivik et al., 2006).

146 Many studies have considered that the most important tectonic event
147 that influenced the NE Atlantic region after breakup occurred around
148 Oligocene time (Talwani and Eldholm, 1977; Lundin and Doré, 2002; Mosar
149 et al., 2002). During that time period, spreading along the Aegir Ridge
150 decreased until it became extinct (around chron 13n) and the spreading
151 axis migrated westwards to initiate the Kolbeinsey Ridge. A change of
152 spreading direction in the Greenland Sea from NNW-SSE to NW-SE led to
153 the fracture zone reorganisation and initiation of the WJMFZ (Talwani and
154 Eldholm, 1977; Lundin and Doré, 2002; Mosar et al., 2002) (Figs. 1, 3). The
155 relocation of the spreading ridge from the aborted Aegir Ridge to the
156 Kolbeinsey Ridge resulted in the separation of the Jan Mayen micro-
157 continent (Nunns, 1982; Unternehr, 1982; Scott et al., 2005) (Figs. 1, 3).

158 3. New data acquisition and processing

159 Our analysis is based on a compilation of old and new, unpublished
160 geophysical data including high-resolution magnetic, ship-tracked
161 bathymetry, gravity, and multichannel seismic profiles provided by
162 the Norwegian Petroleum Directorate (Figs. 2, 4, 5).

A new high-resolution aeromagnetic dataset (JAS-05) was acquired 163
during the autumn of 2005 along the trend of the JMfZ, between the 164
Vøring Marginal High and the Jan Mayen Ridge (Figs. 1, 2). The line and 165
tie-line spacings of the profiles were 5 and 20 km, respectively (Fig. 2b). 166
High-sensitivity measurements, with virtually no drift, were recorded 167
using a modern Geometrics G-822A Cesium Vapor magnetometer with 168
a noise envelope of ± 1 nT. The elevation of the sensor, installed in tail 169
stinger, was c. 230 m. The survey covered a total area of c. 120,000 km² 170
with a total (magnetic) profile distance of 32,600 km. 171

The new raw data have been processed using standard procedures 172
and methodologies followed by other national geological surveys (e.g. 173
Luyendyk, 1997) (Fig. 2). After noise removal, head and lag corrections, 174
the new aeromagnetic survey was processed using a statistical levelling 175
method by which the discrepancies between the readings at each cross- 176
over point (mis-ties and mis-lines) were reduced by systematically 177
proportioning them between the tie and line profiles. 'Suspicious' cross- 178
over differences (outliers) were first removed manually before levelling 179
and full-levelling of the tie and line profiles. The levelling method used 180
for our study involved fitting a polynomial to the intersection errors by 181
the method of least squares (e.g. Mauring et al., 2002). We used a first- 182
order (linear) trend removal for the levelling of the NE-SW tie profiles. 183

Fig. 3. Tectonic calendar of the main tectonic, magmatic and geodynamic events in the Norwegian-Greenland Sea. The chronostratigraphic time scale refers to Cande and Kent, 1995. The NE Atlantic margin tectonic movements, main alpine phases, epeirogenic events, and stepwise subsidence as defined by Praeg et al. (2005). The calendar also shows regionally significant unconformities based on a correlation of megasequences within the NE Atlantic margins from Stoker et al. (2005). Magmatic episodes, rifting and compression along Trill Ø refer to Price et al. (1997). TVIC: Trill-Vøring igneous complex defined by Olesen et al. (2007).

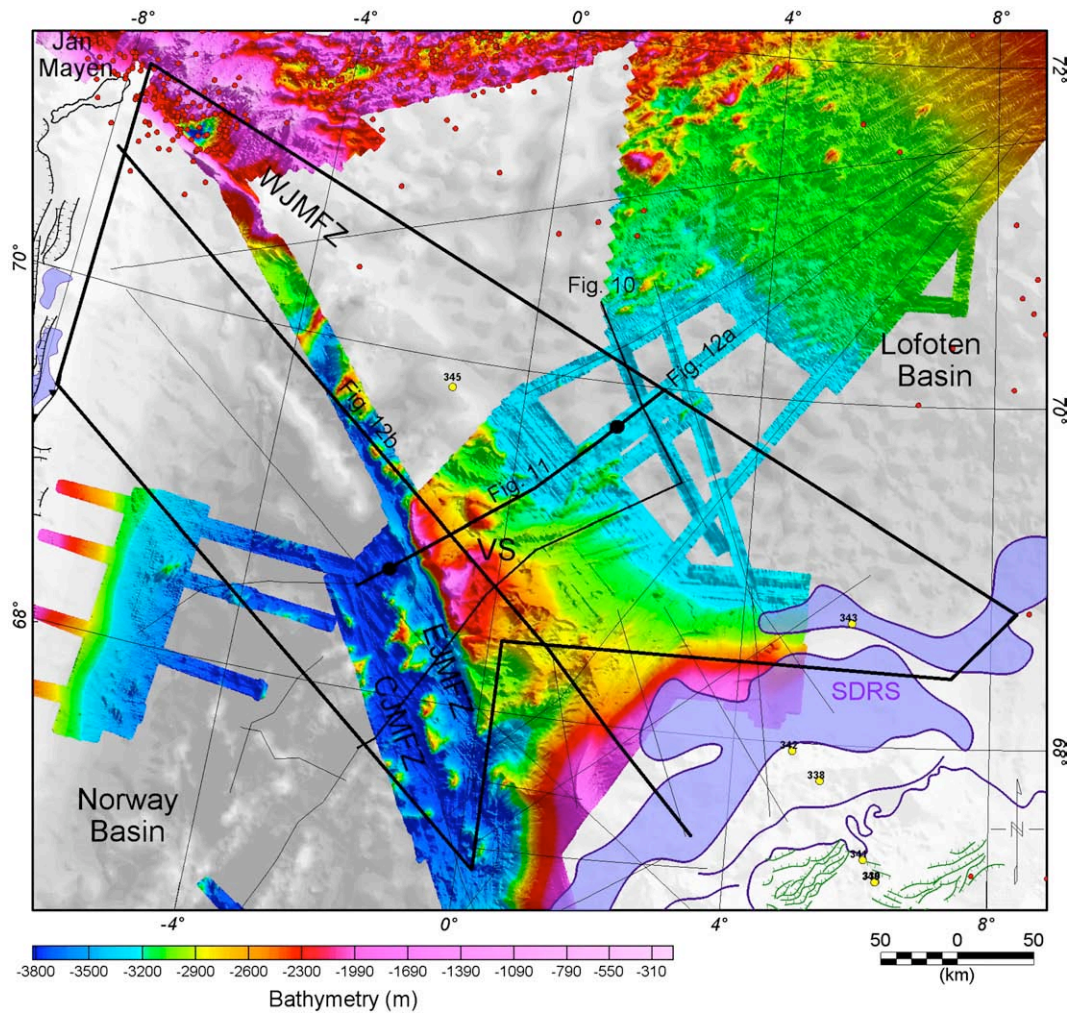


Fig. 5. High resolution bathymetric data merged with bathymetry derived from satellite altimetry (grey background) along the JAS-05 survey area. The Vøring Spur (VS) represents an atypical bathymetric high, located west of the Vøring Marginal High. VS: Vøring Spur.

The linearly trended tie profiles were next used for full statistical levelling of the survey lines after smoothing of the polynomial fitted mis-lines, by means of a spline algorithm, to avoid unwanted distortion of the anomalies (e.g. Mauring et al., 2002). The International Geomagnetic Reference Field (IGRF-2005) was then subtracted from the levelled survey lines to produce the magnetic total field anomalies grid using the minimum curvature technique with a grid cell spacing of 1×1 km.

Finally, the JAS-05 dataset has been merged with pre-existing NGU compilations and systematic adjustment was applied using the minimum curvature suturing function of the Gridknit software (Geosoft, 2005). References and location of the JAS-05 and previous surveys (Fig. 2) are specified in Table 1. Technical description of the vintage profiles and specifications of the previous 5×5 km NGU magnetic compilation are presented in Verhoef et al. (1997) and Olesen et al. (2006, 2007).

The gravity data used in this study are from the regional NGU compilation of Skilbrei et al. (2002) (Fig. 4). This compilation is based offshore on measurements of c. 59,000 km of various shipboard gravity measurements provided by the Norwegian Petroleum Directorate, oil companies, and the Norwegian Mapping Authority. The data were merged with previous Geosat and ERS-1 satellite compilations available in the deep-water areas of the Norwegian–Greenland Sea (Andersen and Knudsen, 1998; Laxon and McAdoo, 1994; Sandwell and Smith, 1997). The surveys have been levelled using the International Standardization Net 1971 (IGSN 71) and the Gravity Formula 1980 for normal gravity. The combined dataset has been interpolated to square cells of 1 km size using the minimum curvature method. We

used a density of 2400 kg m^{-3} to calculate the complete Bouguer correction of the free air anomaly along the survey area (Fig. 8).

Bathymetric data used for the deep-water part of the map (Fig. 5) are based on the satellite altimetry data of Sandwell and Smith (1997). In the JMFZ area, the bathymetry grid has been merged with the multibeam echosounding bathymetric data acquired between 1999 and 2001 by the Gardline Survey contracted by the Norwegian Petroleum Directorate (NPD) (Table 2) (the grid presented in this paper is $1 \text{ km} \times 1 \text{ km}$ (Fig. 5).

Seismic-reflection profiles provided by the NPD were jointly interpreted with gravity and magnetic data (Fig. 4). Some of the vintage multichannel seismic data available in the study area have already been presented by Skogseid and Eldholm (1987). We also obtained access to recent Law of Sea seismic transects acquired by the Gardline Survey and Fugro Geoteam contracted by the NPD in 1999 and 2000. We interpreted and converted the seismic sections using a simple linear V_p velocity versus depth function extrapolated from sea bottom to the top oceanic basement interpreted on the time section. The velocity model ($V_p = 1.90 + 0.43 \times \text{depth}$) refers to a regional compilation presented by Myhre and Eldholm (1980).

4. The Jan Mayen Fault Zone area in the light of the new gridded magnetic data

We have used the new aeromagnetic survey (JAS 05) to re-interpret the position and age of magnetic chrons and the sea-floor spreading history west of the Vøring Marginal High (Fig. 2).

Table 1

Offshore airborne and marine magnetic surveys compiled for the present study (Fig. 2)

Year	Survey areas/references	Operator	Survey name	Sensor elevation (m)	Line spacing (km)
1973	Vøring Basin (Olesen et al., 1997a)	NGU	NGU-73	500	5
1973	South Norwegian–Greenland Sea (Vogt et al., 1979)	NRL	NRL-73	300	10 (20)
1976	Jan Mayen Ridge (CGG, 1977)	CGG/NPD	CGG-76	700	5
1987	Vøring Plateau (Verhoef et al., 1997)	NOO	NOO-87	230	5
1989	Lofoten (Olesen et al., 1997b)	NGU	LAS-89	250	2
1990	Aegir Ridge (Jung and Vogt, 1997)	NRL	NRL-90	0 (ship)	
1993	Hel Graben–Nyk High	WG	SPT-93	80	0.75
2000	Vøring Basin (TGS_NOPEC, 2000)	TGS	VBE-AM-00	130	1–4
2003	Røst Basin (Olesen et al., 2007)	NGU	RAS-03	230	2
2005	Jan Mayen FZ (Olesen et al., 2006)	NGU/TGS	JAS-05	230	5
2007	Norway Basin (Gernigon et al., 2008)	NGU	NB-07	230	5

CGG – Compagnie Générale de Géophysique; NOO – Naval Oceanographic Office; NGU – Geological Survey of Norway; NPD – Norwegian Petroleum Directorate; NRL – Naval Research Laboratory; TGS – TGS NOPEC Geophysical Company; WG: World Geosciences.

The total field magnetic grid contains signals with a wide range of amplitudes, reflecting the varying depth, geometry and susceptibility contrasts of sources. The TDX normalised filtering technique (Cooper and Cowan, 2006) was used in this study to identify magnetic reversal sequences (Fig. 6, 7). The TDX filter of the JAS-05 magnetic grid $M(x,y,z)$ is defined by:

$$TDX = \tan^{-1} \left(\sqrt{\frac{(\partial M/\partial x)^2 + (\partial M/\partial y)^2}{|\partial M/\partial z|}} \right)$$

The problem to be overcome in data enhancement using the TDX filter was to identify and map subtle anomalies attenuated in the dynamic range due to the presence of high-amplitude magnetic anomalies, the continuity of individual bodies and the edges of structures. Combined and merged with the original grid, the filtered grid has been used to highlight and pick the inflection points on both edges of the anomalies (Figs. 6, 7). The new magnetic chrons have been interpreted with reference to the chronostratigraphic time scale of Cande and Kent (1995) (see selected profiles in Fig. 7) and their interpretation of the magnetic chrons has been correlated with synthetic profiles calculated using the forward modelling method of fictitious spreading rate (Mendel et al., 2005) and assuming a constant spreading direction (Fig. 7). The interpretation of the Aegir Ridge NRL-90 magnetic survey by Jung and Vogt (1997) and the work of Tsikalas et al. (2002) and Olesen et al. (2007) have been considered as the most recent and reliable guides to reassess the chrons interpretation on the JAS-05 survey area.

The JMFZ represents a broad zone and consists of three distinct segments respectively named the western, eastern and central Jan Mayen fractures zones (WJMFZ, EJMFZ, CJMFZ) (Fig. 1) (Blystad et al., 1995). These segments are characterised by large-scale basement reliefs forming elongated ridges and troughs with associated gravity anomalies (Figs. 1, 4). They are very well-observed in the new aeromagnetic compilation (Figs. 2, 6). The main fracture zones are located in regions where the magnetic anomalies are offset and they present NW–SE elongated patterns with usually low magnetic signatures which could reflect the destruction and mechanical disorganisation and/or chemical demagnetization of the topmost part of the oceanic crust (Fig. 2d). The EMFZ and CJMFZ run sub-parallel to each other across the northern part of the Norway Basin and the magnetic trends suggest a change from N130° at its western end to about N°150 at its eastern end.

The signature of the EJMFZ is the most distinguishable on the new grid and the traces of the CJMFZ and WJMFZ correspond to net offsets and local displacement of the magnetic chrons (Figs. 2d, 6). The magnetic trace of the WJMFZ with an azimuth of 110°N includes the modern active transform offsetting the Mohns Ridge to the north and the Kolbeinsey Ridge to the south. The WJMFZ was previously interpreted to extend only up to magnetic chron C13 as suggested by the vintage dataset (Lundin and Doré, 2002). Our current interpretation suggests that an amalgam of discrete fracture zones existed between C21 and C19 in the eastern prolongation of the WJMFZ. This transition zone between the VS and the Lofoten Basin is highly disrupted by oblique faulting and block dislocation (Figs. 2, 6).

The western part of the JAS-05 survey covers the rift to drift transition of the East Jan Mayen margin (Figs. 2, 6, 7). Gudlaugsson et al. (1988) and Skogseid and Eldholm (1987) previously described a system of rotated blocks and seismic wedges interpreted as volcanic SDRs. However, volcanic SDRs are missing along the conjugate system, south of the EJMFZ (Berndt et al., 2001a) raising concerns about the nature of the dipping wedges observed along the northeastern margin of the Jan Mayen Ridge. These wedges could correspond to composite structures involving minor lava flows above underlying rotated and tilted sedimentary blocks instead of massive volcanic flood basalts emplaced along the breakup axis (SDRs, strictly speaking). East of these wedges and south of the EJMFZ, the magnetic signature has been interpreted as oceanic crust C24B to C13n. The half-spreading rates estimated from the new magnetic dataset are 22 to 18±2 mm/year between C24B and C21n, and 10 to 6±2 mm/year between C21n and C18n. Between C18n and C13n, the half-spreading rate was still low but had increased slightly to 11±2 mm/year (Fig. 7). Landward of C24A, the reverse C24r may eventually represent the COB, the limit between the real oceanic domain and the continent–ocean transition zone (Figs. 2, 6, 7). Positive anomalies before C24B may possibly represent intrusions and/or volcanic rocks emplaced along the continental–ocean transition between C26n and C25n.

Magnetic chrons C24B and C24A have been identified along the eastern margin of the Jan Mayen microcontinent, but the double 24A and 24B chron system between the Jan Mayen Ridge and the Vøring Marginal High has not been observed on the new dataset, thus questioning the previous interpretation of an aborted ridge at C24 (Skogseid and Eldholm, 1987). We point out that recent magmatic activity on Jan Mayen island may also have influenced the magnetic signature in the western part of the survey and could have affected the initial pattern. A closer look at the pre-existing data suggests that along most of the Vøring Marginal High, the magnetic signature is strongly influenced by the volcanic flows emplaced all along the continent–ocean transition (Figs. 2, 6, 7). It cannot be excluded that most of the earliest linear anomalies observed both along the Vøring Marginal High and along the eastern flank of the Jan Mayen Ridge may simply represent the tilt and/or faulting effects of thick and magnetic lava units and/or dyke or mafic intrusions plumbing the continental and/or transitional crust, as observed onshore East Greenland (Geoffroy, 2005).

West of the extinct Aegir Ridge, the western segment of the CJMFZ is better defined on the JAS-05 grid as suggested by the dextral shift and curved pattern of the magnetic chrons from C24 to C19n–16n (Figs. 2, 6). They fit a conjugate pattern, similar to that observed in the southern corner of the Vøring Marginal High. Between the EJMFZ and the CJMFZ, curved magnetic anomalies from C24B to C16n probably reflect the passive effects of local deviatoric stress reorientation close to the main fault zone.

In addition, new anomalies are clearly observed between the central part of the survey area north of the EJMFZ from C23n to C13n. DSDP well 345, located in the central part of the survey area, is located at the level of magnetic chron C18n (40.13–38.42 Ma) and provides a good age constraint for the oceanic basement (Figs. 6, 7). Our interpretation of the magnetic chrons is in good agreement with the 48–41 Ma age range of the oldest sediments recovered from the drillcore of DSDP well 345 (Goll, 1989). To the west, younger and new anomalies are observed up to C5 between the EJMFZ and the WJMFZ. However, their identification

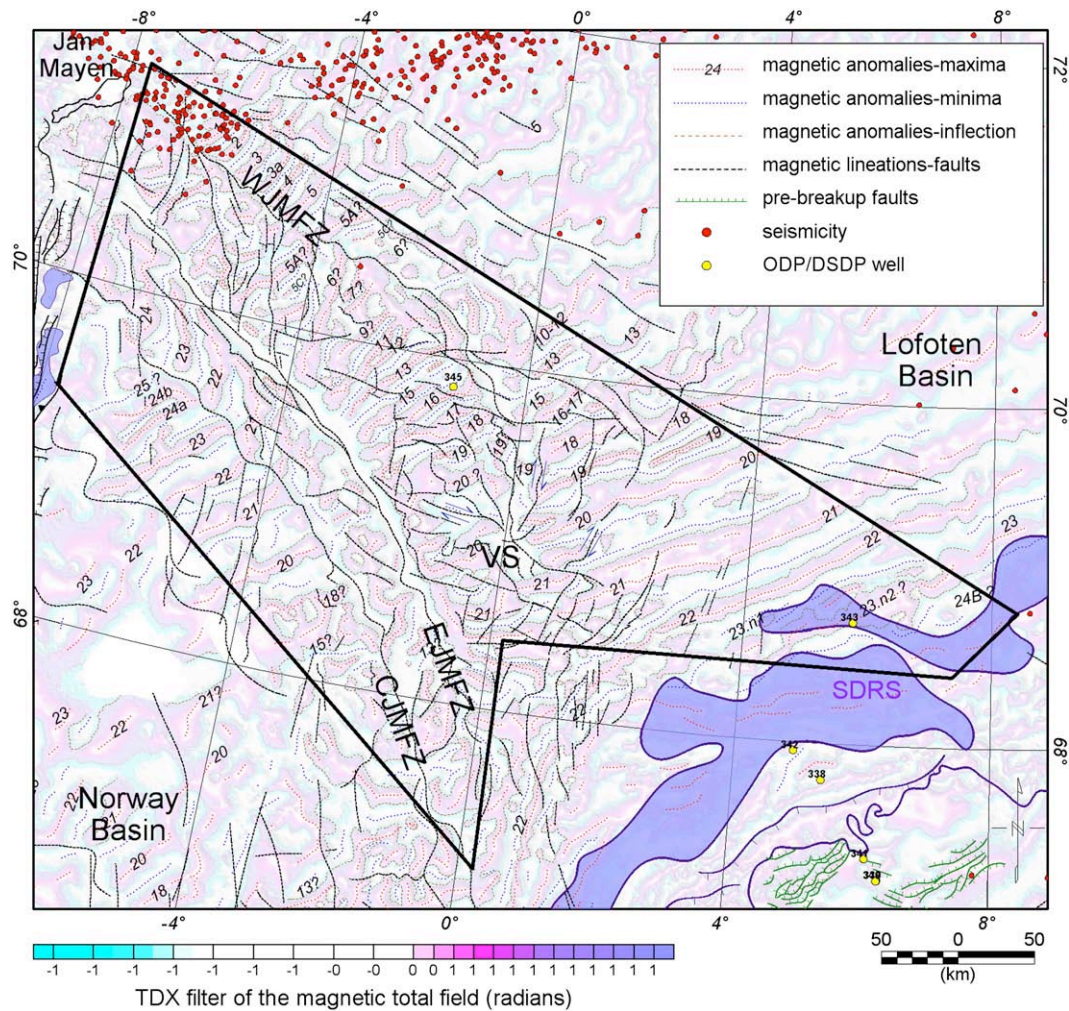


Fig. 6. TDX filter of the magnetic total field and overlying interpretation of the magnetic anomalies. The dashed lines represent maximum, minima and inflection points detected for each magnetic anomaly. The map also shows the main magnetic lineaments and chrons have been interpreted with reference to the chronostratigraphic time scale of [Cande and Kent, \(1995\)](#). VS: Vøring Spur.

remains relatively uncertain due to local faulting, block dislocation and possibly late intrusions or volcanic rocks near Jan Mayen island.

To the west, normal and reverse magnetic stripes are better recognised west of the Vøring Marginal High, between C23n and C18n–C16n (Figs. 2, 6, 7). Close to VS, the magnetic pattern from C23n (51.7–50.7 Ma) to C20n fits the southern prolongation of the magnetic stripes previously identified in the Lofoten Basin (Tsikalas et al., 2002; Olesen et al., 2007). Half-spreading rates vary from 36 to 17.6 mm/year between C24B and C20n and slightly increase from 10.6 to 11.8 mm/year between C20n (43.78–42.53 Ma) and C13n (Fig. 7). The magnetic pattern suggests apparent shifts of magnetic chrons in the northern part of the JMZF, indicating that local stress reorganisation along the Lofoten Basin could have started before C13n and most likely after C21n (Figs. 2, 6, 7). This is visible west of the C21n by the shift of the C19n anomaly and the highly deformed oceanic (magnetic) basement between C21n and C20n north of the VS (Figs. 2, 6). An apparent shift of the C21n anomaly is notably observed close to the VS and suggests strike-slip displacement and dislocation of the oceanic crust, accommodated by N–S faults, in Early Eocene time. In the Lofoten Basin, the magnetic chrons suggest a NW–SE spreading direction (N°150), but south of the VS the anomalies between C23n and C21n rather suggest a N°100–120 direction (Figs. 2, 6). This difference of 50° is probably explained by two regional stress directions that interacted near the VS and led to faulting and block rotation. Discrete N–S lineaments interpreted as faults on the new gridded data (Fig. 6) could be related to a more complex plate motion history and local reorganisation of plate boundaries around the Jan Mayen microcontinent (Gaina et al., submitted).

North of the WJMFZ, the youngest spreading system from C5n to C1 364 in the southern part of the Mohs Ridge is also well-defined on the new 365 dataset (Figs. 2, 6, 7). This area is still seismically active and spreading 366 rates vary between 8 and 6 ± 2 mm/year (Fig. 7). 367

5. The Vøring Spur (VS): an intriguing oceanic feature of the 368 Norwegian–Greenland Sea 369

5.1. Stratigraphy and shallow structures of the Vøring Spur 370

The VS is an unusual bathymetric high located along the trend of 371 the JMZF (Figs. 1, 5). The magnetic striped pattern suggests that this 372 atypical bathymetric high is most likely an oceanic feature situated 373 between chrons C21r and C13n on the northern prolongation of the 374 aborted Aegir Ridge (Figs. 2, 6, 7). The VS coincides with a clear gravity 375 low (Fig. 8, 10) and is well-recognised in the magnetic data (Figs. 2, 9). It 376 is clearly asymmetric with a steep slope on the EJMFZ side and a 377 smoother slope towards of the north (Figs. 10, 11). North of the VS, 378 major bounding faults can be observed on seismic profiles and fit with 379 the dislocated fault zone observed east of the WJMF. Individual 380 basement blocks observed can be correlated with the gravity and 381 magnetic anomalies. 382

Affected by normal faulting, the sedimentary package imaged between 383 the VS and the Lofoten Basin has been subdivided into two major and 384 distinct seismic units (Units I and II), separated by a regional unconformity 385 (U1), which extends through most of the Lofoten Basin (Figs. 10, 11). 386

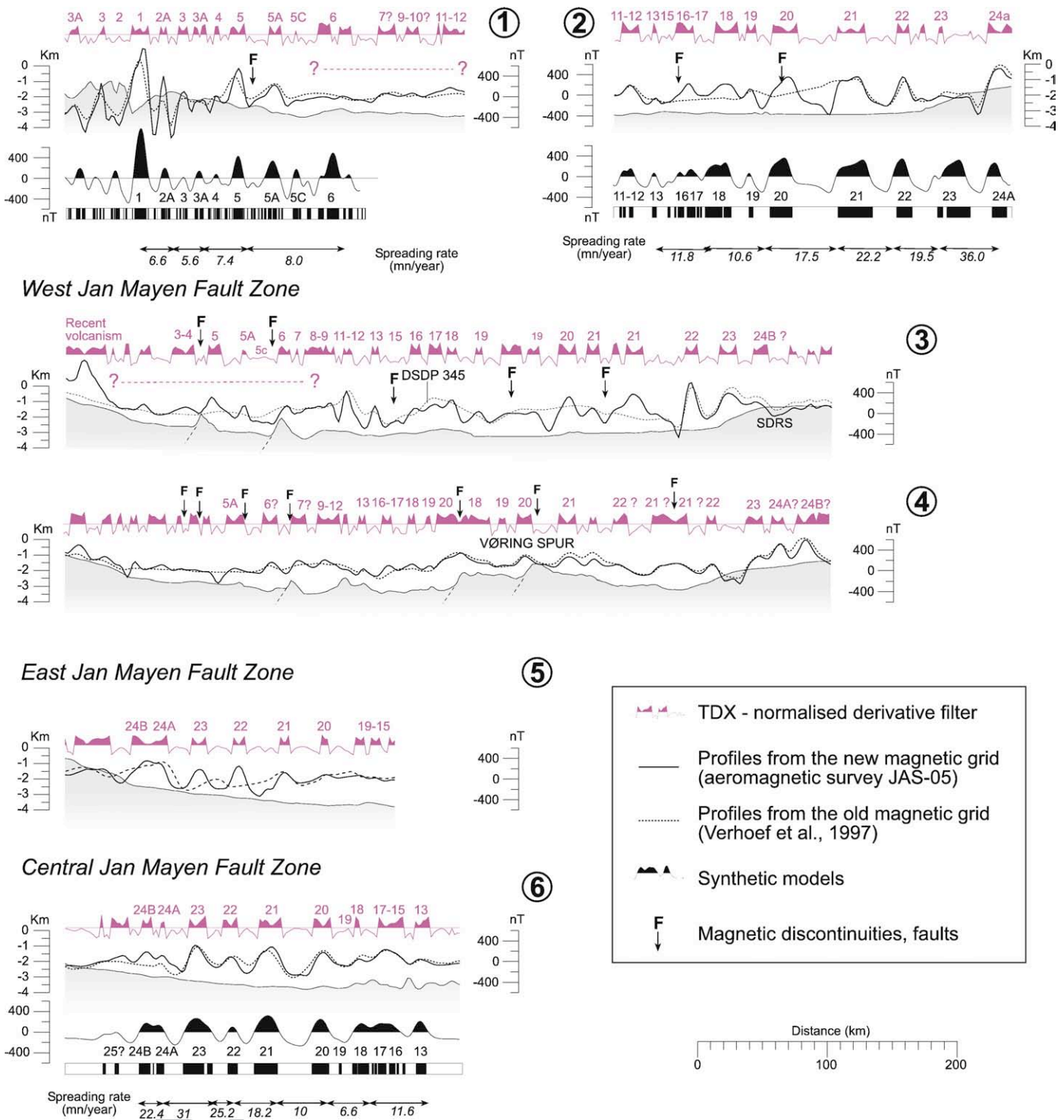


Fig. 7. Selected bathymetric and magnetic transects across the JAS-05 survey area. The interpretation of the magnetic chrons has been correlated with synthetic profiles calculated using the forward modelling method of fictitious spreading rate and assuming a constant spreading direction. See Fig. 2 for location.

387 Unit II forms a distinct seismic package with variable, semi-
 388 continuous, low-amplitude markers. Close to the main fault zones, the
 389 facies is locally disorganised, discontinuous and sometimes chaotic
 390 and transparent (Fig. 11). Along the VS, Unit II represents a thick
 391 sedimentary package on top of a high structure, but identification of
 392 the sub-sequences is unclear due to chaotic and disorganised seismic
 393 patterns. On the northern flank and on top of the VS, moats, lenticular,
 394 upward-convex units and downlapping and sigmoidal progradational
 395 reflectors have been observed (Fig. 10).

Unit I represents a uniform seismic package with clear, continuous, 396
 sub-parallel high-amplitude reflections alternating with continuous 397
 low-amplitude, high frequency reflectors. Unit I can reach a thickness 398
 of 1000 m in the Lofoten Basin but thins and pinches out on the 399
 northern flank of the VS. Compared to Unit II, only minor faulting 400
 affects Unit II. Nonetheless, minor movements due to reactivation of 401
 deeper underlying faults are observed and seem to accommodate 402
 growth wedges and synformal structures, which show that faulting 403
 was still active even during and after the development of U1 (Fig. 11). 404

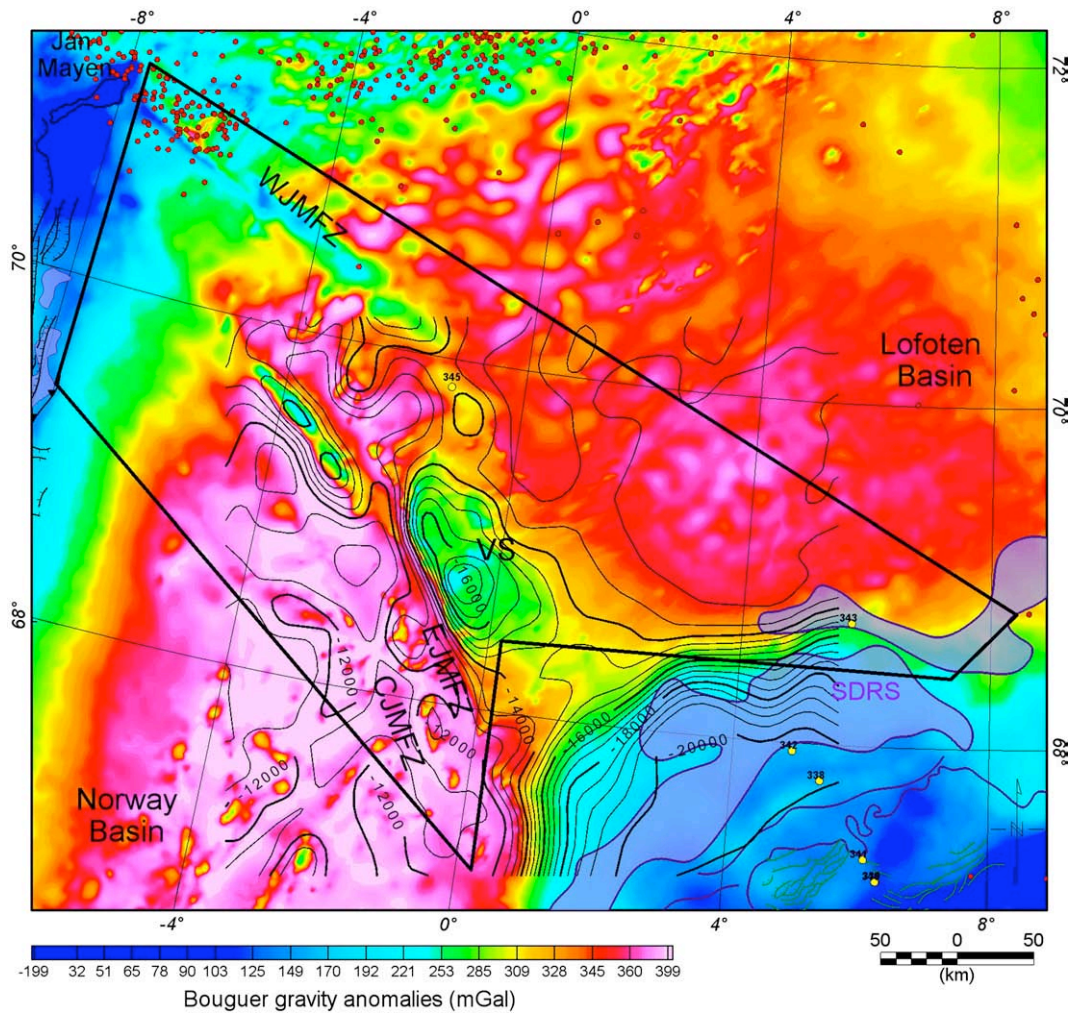


Fig. 8. Bouguer anomalies map combined with depth contours of the flexural Moho estimated for low elastic thickness ($T_e = 1$ km). The Vøring Spur (VS) is characterised by an apparent Bouguer low, contrasting with the surrounding oceanic domains. The gravity low coincides with a thick oceanic crust (> 15 km) between the Lofoten and Norway Basins.

Some uncertainties exist about the nature and age of the sequences described along the JAS-05 survey area. A direct calibration of the seismic sequences by well DSDP 345 and other drillholes was not feasible in this study due to low seismic coverage and pinch-out of the Cenozoic sequences around the Vøring Marginal High. However, the sedimentary sequences and the regional unconformity, described here, tend to reflect major phases of basin evolution, commonly a response to major geodynamic changes, which modified sedimentary patterns and paleo-oceanographic circulation.

The thick sedimentary package on top of the VS does not necessarily point to any depocentre inversion, but can simply reflect upslope-accreting pelagic and contourite sediments deposited on the flanks and top of a pre-existing oceanic high (Figs. 10, 11). Sigmoidal and erosional lenticular, upwardly convex seismic patterns support the interpretation of contourite drifts (sensu Faugères et al., 1999) around the VS (Figs. 10, 11). Such drifts probably initiated in Miocene time (Fig. 3), as previously described along the Mid-Norwegian shelf (Laberg et al., 2001).

A combination of seismic profiles, together with the new JAS-05 magnetic data provides some constraints for dating the different seismic units. The seismic features can be correlated with the magnetic chrons and provide a means to establish the chronostratigraphy of the oceanic basement and overlying sequences (Fig. 10).

U1 can be followed on top of the oceanic crust at least up to C12n, as identified on the JAS-05. We concluded that the sediments of Unit I are definitively older than latest Oligocene. Due to low seismic coverage after

C12n, we were not able to determine if these markers are present after chron C12n. However, Breivik et al. (2008) have published new seismic profiles north of our study area showing that this major unconformity clearly extends up to magnetic chrons C6–C5 (Early to Mid-Miocene). By inference, sediments of Unit II are interpreted to be Late Miocene or younger. This unconformity could eventually correlate with the base Pliocene described farther north along the Barents Shelf by Hjelstuen et al. (2007) (J. Skogseid, pers. comm., 2008). U1 could represent a prolonged hiatus and unconformity spanning from early Late Miocene to Pliocene.

6. Gravity modelling and deep crustal architecture of the VS

To help elucidate regional variations in bathymetry and crustal structure of the VS, a 2.5 forward modelling was carried out in the survey area (Fig. 12). A Transect 1 was modelled using a NW–SE seismic line across the VS (Fig. 12a) and a NW–SE regional transect (Transect 2) covers the survey area from the Vøring Marginal High to Jan Mayen (Fig. 12b).

Moho depths have also been independently computed using the ASEP algorithm of Wienecke et al. (2007) (Fig. 8). This algorithm allowed us to compute a 3-dimensional analytical solution, which described the flexure of a thin elastic plate with a higher spatial resolution than conventional spectral methods. We estimated the 3D shape of the Moho around the VS assuming a different elastic-plate thickness (T_e), an average crust density of 2850 kg m^{-3} and a mantle density of 3200 kg m^{-3} . From the geophysical grids, we extracted theoretical flexural Moho profiles, for comparison

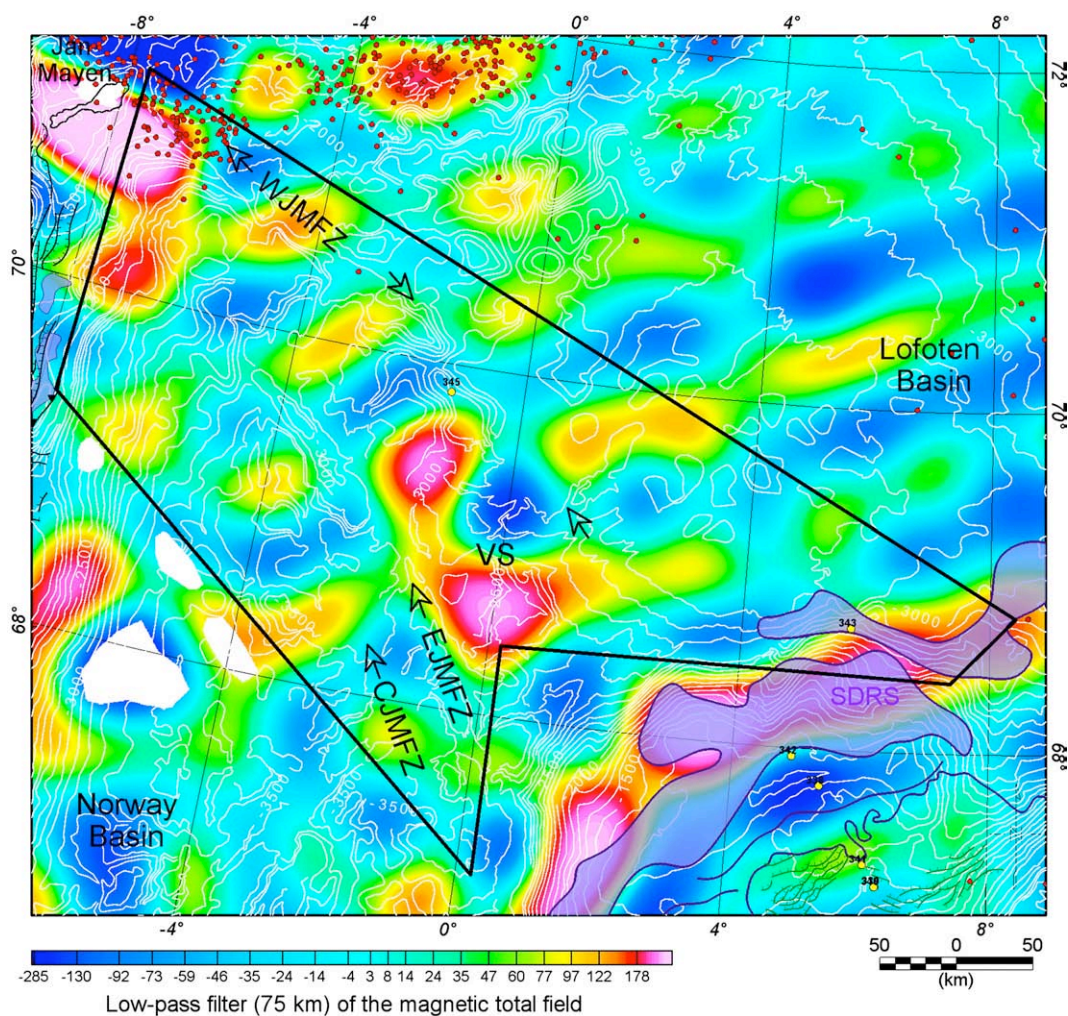


Fig. 9. Low-pass filter (75 km) of the new magnetic total field. The Vøring Spur (VS) and the overcrusting area also coincides with positive long-wavelengths on the magnetic total field relatively similar to those observed close to the Seaward Dipping reflectors (SDRS) and around the Jan Mayen Island. The long-wavelengths might reflect the combined effect of the shallow top basement and deeper magnetic sources. Also, note that the main fracture zones (arrows) represent shifts of the long- to medium-wavelengths revealed by this map. The white contours represent the bathymetry.

with the forward models constrained by the seismic profiles (Fig. 12). The best Moho estimation around the VS was derived from the best-fitting flexural model obtained with $T_e = 1$ km which, by definition, is close to the Airy approximation (Figs. 8, 12). Between the Vøring Marginal High and the VS, a V-shaped bathymetric low is observed with changes from lower to higher gravity anomalies (Fig. 8, 12b). It coincides with a shallowing of the Moho, west of the thick underplated crust observed on the continent-ocean transition (Fig. 12b). To the west, a deeper Moho was deduced by our modelling on the VS and fits the result of the Ocean Bottom Seismometer (OBS) experiment 11-2003 published by Breivik et al. (2008).

The two gravity modelling approaches suggest that the broad gravity low in the close vicinity of the VS is not only due to the bathymetric anomaly, but is also influenced by the presence of a deep crustal root, suggesting isostatic compensation. The thick oceanic crust beneath the VS is interpreted as mafic and we note that this thickening is almost similar in size to the lower crustal body modelled underneath the Vøring Marginal High (Fig. 12) (e.g. Breivik et al., 2008; Mjelde et al., 2007). A thick oceanic crust of approximately 16–17 km beneath the VS comes as a surprise for the reason that the common and 'normal' oceanic crustal thickness usually does not exceed 7–10 km on average (White et al., 1992). The main explanations for such a thick oceanic crust and formation of the lower crustal root involve either 1) anomalous melt accumulation, emplaced beneath the VS during the ridge accretion, or 2) a late and post-rift underplating that accumulated under the pre-existing crust as favoured by

Breivik et al. (2008). The thick crust is observed between magnetic anomalies C22n and C18n and, in both case, the two interpretations agree upon an anomalous and major post-breakup melt production. To avoid any later confusion with the Late Miocene underplating hypothesis of Breivik et al. (2008), we refer by the term of 'overcrusting' to the favoured process involving an anomalous but syn-spreading magmatic production.

7. Uplift of the Vøring Spur: local and regional considerations

The structure and sedimentary record in the vicinity of the VS clearly show that it was affected by vertical motions, locally controlled by faults. Comparing the seismic structure with the square root model of Parsons and Sclater (1977), we show that the VS rises 1000 to 1500 m above normal (theoretical) oceanic crust of the same age predicted by the isostatic model (Fig. 12a). This difference also coincides with the length of the apparent throw observed along the EJMFZ and has been considered as the apparent uplift of the VS.

7.1. Airy considerations

The crustal root underlying the VS is likely to have influenced the surface expression of this atypical oceanic feature (Figs. 5, 10, 11). The classic Airy model of local isostasy assumes that the upper part of the lithosphere is balanced hydrostatically and cannot support any deviatoric

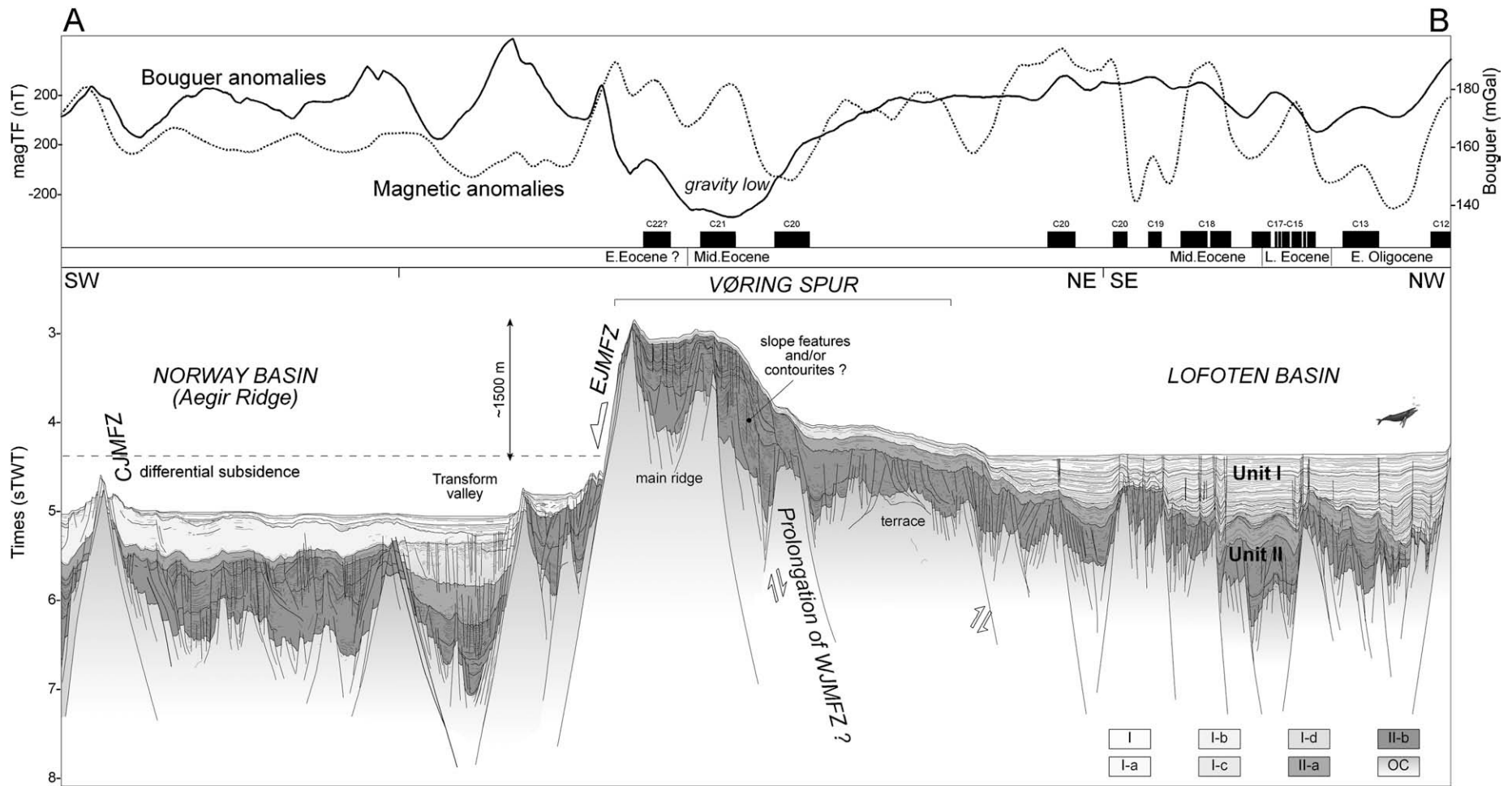


Fig. 10. Composite transect and observed gravity and magnetic profiles across the Vøring Spur (VS) and Lofoten Basin (location on Fig. 4). The oceanic crust in the Lofoten Basin accreted between chrons C20n (43 Ma) and C12n (31 Ma), underlined by the magnetic total field anomalies. C13n marks the Eocene–Oligocene transition according to the geomagnetic polarity time scale of Cande and Kent (1995). The transect illustrates the asymmetric structure of the VS controlled by the EJMfz. The southeastern part of the VS divides between a narrow (75 km) ridge, near the EJMfz and an adjacent terrace, 100 km wide, making the ridge's transition to the Lofoten Basin. To the northwest, the main ridge is characterised by two separate blocks and the terrace appears as a separate block. This transect also illustrates the main seismic units (Units I and II) and their sub-sequences discussed in the text. See Figs. 4 and 5 for location.

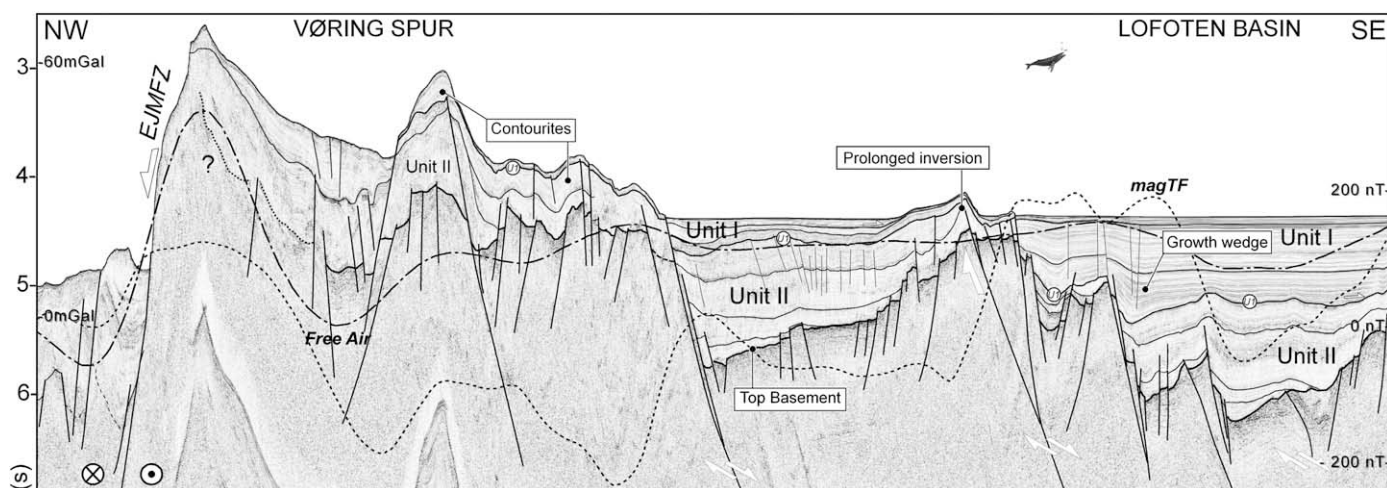


Fig. 11. Profile across the Vøring Spur based on the interpretation of the NPD-LOS99-006 seismic line (see Fig. 5). This example illustrates the seismic characteristics of the VS and its long-lived period of fault activity. Faulting started before the main uplift between Units I and II separated by the regional unconformity U1 (Miocene in age). Forced folding features and growth wedges can be observed in Unit 1 and suggest late reactivation (Miocene–Recent) and rotation of pre-existing hanging-walls.

497 stress. If we consider the best density parameters deduced from the
 498 forward modelling, and an average density between 2800 and 2900 kg/m³,
 499 the Airy model explains uplifts of up to 1000 m (Fig. 13). This simple
 500 calculation suggests that, the apparent uplift observed at the VS can simply
 501 be explained by an isostatic effect of the overcrusting deduced both by
 502 gravity modelling and by recent OBS observations (Breivik et al., 2008).

503 7.2. Tectonic alternatives

504 The strong asymmetry of the VS suggests that the EJMfZ exerted some
 505 control during the uplift (Figs. 10, 11, 13). Even if Airy conditions VS rule at
 506 present day, we cannot exclude that higher rigidity might have existed in
 507 the past. The shape of the VS could have been controlled by a mechanical
 508 flexural flank uplift accommodated by the EJMfZ. We considered that an
 509 upward flexure of the edge of a weak lithospheric elastic plate, accom-
 510 modated by the EJMfZ, could have been one of the mechanisms involved in
 511 the vertical motion of the VS (Fig. 13). Similar asymmetric transverse
 512 ridges and flexural mechanisms have been described along many other
 513 intra-oceanic transforms (Wessel and Haxby, 1990), and observations and
 514 modelling have showed that significant (>1 km) tectonic uplift associated
 515 with transform faults is commonly recognised (Baines et al., 2003; Bonatti
 516 et al., 1994). To test this hypothesis, we used the approximation of Bullard
 Q4517 (Watts, 2001), a simple equation, that links the deflection of a thin elastic
 518 plate and its elastic thickness with the geometry of a major border fault
 519 (the EJMfZ) and its median valley:

$$520 T_e = \sqrt[3]{\frac{3 \cdot 4^3 (\rho_{MI} - \rho_{Infill}) \cdot g \cdot x_0^4}{E \cdot \pi^4}}$$

521 with

522 $E = 1011 \text{ Pa}$: Young's modulus

523 $g = 9.81 \text{ m} \cdot \text{s}^{-2}$: gravity

524 $\rho_{MI} = 3200 \text{ kg} \cdot \text{m}^{-3}$: mantle density

525 $\rho_{Infill} = 2000\text{--}2100 \text{ kg} \cdot \text{m}^{-3}$: infill density of sediments

526 x_0 represents the distance between the main border faults and its
 527 conjugate as described on Fig. 13a.

528 Taking into consideration a NE–SW profile across the VS, the main
 529 border fault could represent the EJMfZ and the bathymetric scarp,
 530 highlighted by the CJMfZ and located at distance x_0 interpreted as the
 531 conjugate fault system of the broken plate (Fig. 13d). Using the Bullard
 532 relationship, we estimated a potential elastic thickness of the litho-
 533 sphere and we obtained a value for the elastic thickness T_e of 10–13 km,

534 which agrees with similar predicted values for oceanic crust younger
 535 than 50 Ma (Watts, 2001). The flexure of a broken plate could be pro-
 536 posed as a viable alternative to explain the geometry and uplift of the VS
 537 (Fig. 13). The low T_e along the VS fits with the Airy model at present day,
 538 but could have been higher at some stage or could simply represent the
 539 localised weakness zone of the broken plate region (Fig. 13d). Normal
 540 stress along the pre-existing EJMfZ could have explained the episodic
 541 tectonic flank uplift and block tilting observed around the VS that lasted
 542 up to recent times.

543 For intra-oceanic fractures zone, differential thermal subsidence on
 544 either side of the fault zone is also a tectonic process which has com-
 545 monly been suggested to explain the presence of transverse ridges
 546 near oceanic transforms (Bonatti et al., 1994). After abortion of the
 547 Aegir Ridge, slightly before C7 (25.64–24.73 Ma), the cooling of the
 548 oceanic crust located south of the EJMfZ is likely to have influenced the
 549 differential subsidence on either side of the EJMfZ (Fig. 14). During
 550 Oligocene–Miocene time, the Aegir Ridge also accreted to the south
 551 and close to the VS (Fig. 14). During that period, lateral heat transfer
 552 between the hot lithosphere along the Aegir Ridge and the adjacent
 553 cooling plate could have influenced the vertical motion of the VS, as
 554 suggested by the modelling of Chen, (1988). Hydration–dehydration
 555 reactions along the main fractures zone can also influence vertical
 556 motions, but only to a limited extent (Bonatti et al., 1994). These
 557 mechanisms are not mutually exclusive, but should be treated in a
 558 unified manner. The uplift of the VS probably involved several
 559 interacting processes, including flank uplift driven by far-field normal
 560 stress, heat transfer and subsequent differential thermal subsidence
 561 after abortion of the Aegir Ridge, and the increasing buoyancy effect of
 562 the overcrusting that developed earlier in Eocene time (Fig. 14).

563 The main unconformity (U1) may reflect a major tectonic reactivation
 564 of the VS in the Late Miocene as a consequence of the stress regime
 565 modification along the EJMfZ, but U1 also coincides with a major change
 566 of the sedimentary environment at the regional scale, e.g. the Lofoten
 567 Basin, as far as 350 km from the VS itself (e.g. Breivik et al., 2008; Hjelstuen
 568 et al., 2007). Coeval uplift and subsidence during Late Neogene time has
 569 previously been recognised from onshore to offshore correlations on the
 570 Norwegian margin (Stuevold and Eldholm, 1996), but uncertainties have
 571 surrounded the timing of events, with estimates of the onset of uplift
 572 ranging from Oligocene to Pleistocene, mainly due to controversial
 573 interpretations of the stratigraphy of the inner Norwegian margin
 574 (Henriksen and Vorren, 1996). The disputed uplift is now recognised to
 575 be not older than latest Miocene (Bugge et al., 2004), consistent with the

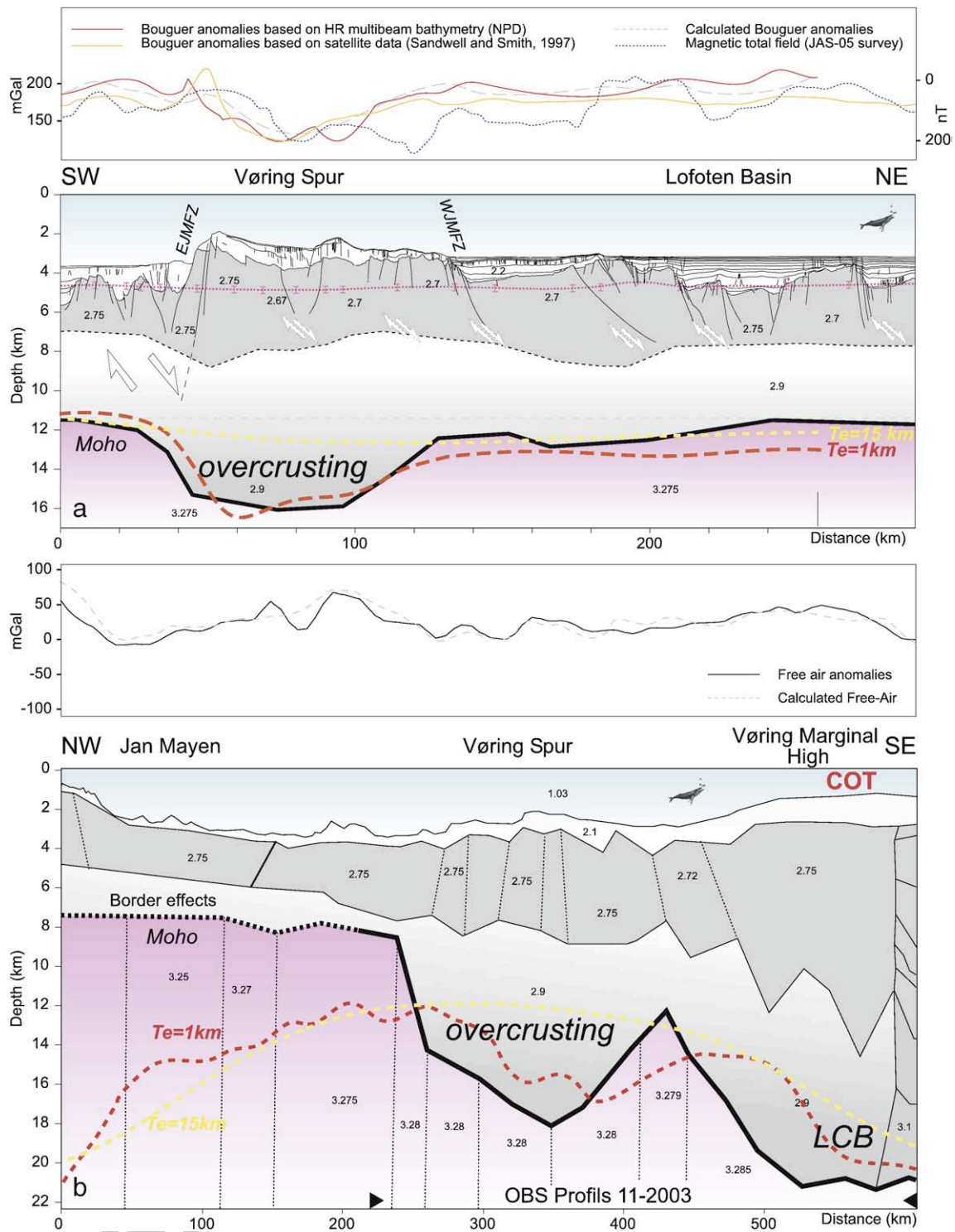


Fig. 12. Gravity forward modelling and crustal model across the Vøring Spur (location on Fig. 4). a) NE-SW Transect 1 along the NPD-LOS99-006, provided by the Norwegian Petroleum Directorate. Density values are indicated in g cm^{-3} . Theoretical depth of the top oceanic basement (uppermost dashed line) has been calculated using the empirical depth (D) versus ages (t) square [$D(t) = Ct/2 + D(t=0)$]. The magnetic grid has been used to constrain ages of the basement and we applied a subsidence factor C of $250 \text{ m/Ma}^{1/2}$. The curve shows that the current location of the top basement along the VS does not fit with the theoretical predicted model for a magma-rich oceanic system. b) NW-SE Transect 2 along the seismic line NPD-NH79 from the Vøring Marginal High to the Jan Mayen Ridge. The upper panel shows the modelled and observed gravity and the lower panel the density structure. Deep dashed lines represent different flexural Mohos assuming respectively plate elastic thicknesses (T_e) of 15 and 1 km along the two transects. The oceanic root, observed beneath the VS, is interpreted as a syn-rift oceanic and mafic feature (so-called overcrusting) formed during Mid-Late Eocene time.

576 expected age of the main unconformity U1 and the onset of major fan
577 development on the Barents Sea margin (Hjelstuen et al., 2007). This event
578 is coeval with an acceleration of subsidence and the onset of continental
579 glaciation recognised around other North Atlantic margins (Fig. 3) (Stoker

et al., 2005). Comparable vertical motions of a similar age observed at the
580 scale of the North Atlantic cannot simply be a consequence of the local
581 uplift of the VS alone but could represent the response of larger geological
582 and complex geodynamic changes, as discussed at the scale of the entire
583

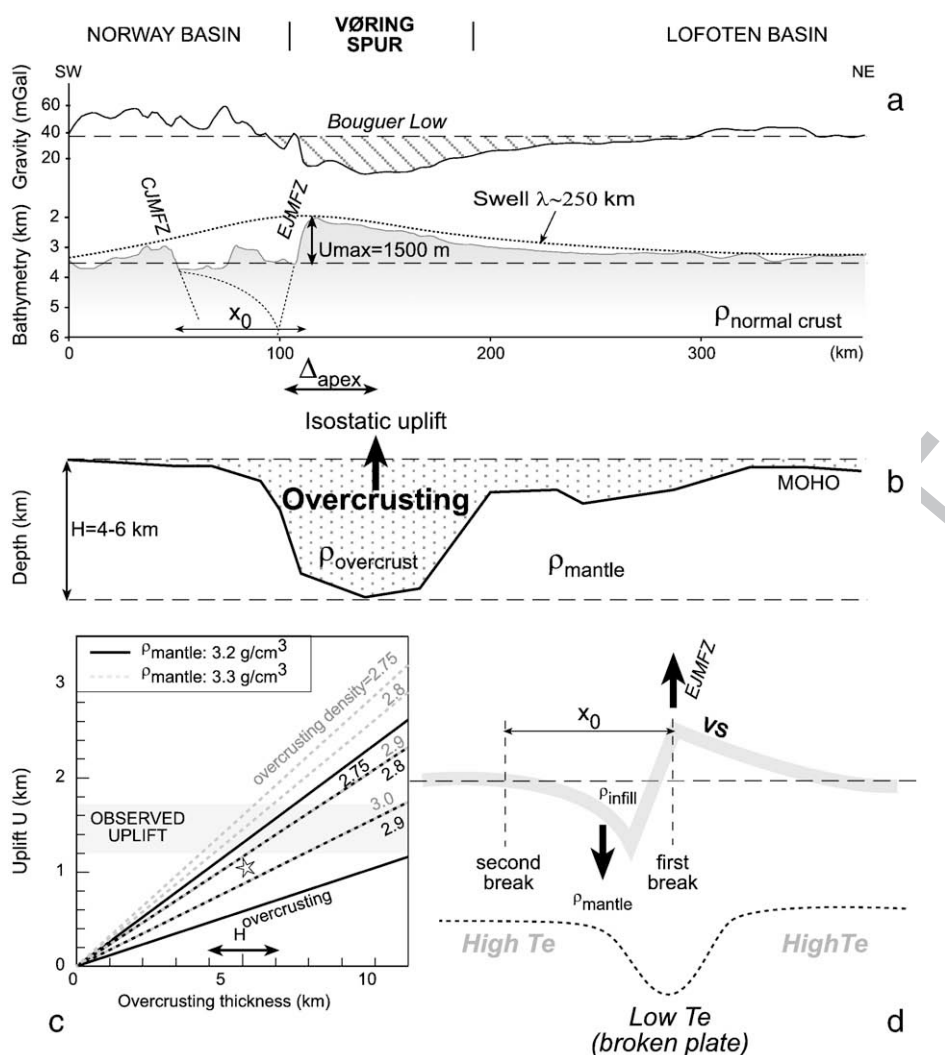


Fig. 13. Interplay between the oceanic high and the overcrusting observed underneath the VS. a) NE-SW bathymetric and Bouguer gravity profiles across VS. The Bouguer low anomaly coincides with the overcrusting (b) but the maximum amplitude of the rough swell due to VS uplift (dot line) does not exactly fit the apex of the deep root. c) Estimated isostatic uplift due to crustal thickening and comparison between the predicted versus observed uplift. Assuming that VS stayed beneath sea level, the maximum uplift U generated by emplacement of the overcrusting, with a thickness H , was approximated by $U = H (\rho_{mantle} - \rho_{overcrusting}) / (\rho_{normal\ crust} - \rho_{water})$. This simple assumption neglects flexural and denudation effects and provides isostatic values obtained using a reasonable range of overcrusting densities $\rho_{overcrusting}$ (2750 to 3000 kg/m³) and mantle density ρ_{mantle} (3200 to 3300 kg/m³). The star represents the parameters deduced from the forward modelling. d) Rift flank uplift model controlled by the EJMfz. This flexural model could explain the asymmetry and the tectonic uplift of the VS.

584 North Atlantic by Praeg et al. (2005) (Fig. 3). As a result, we cannot
 585 conclude that a direct and exclusive genetic relationship exists between
 586 the major unconformity U1 and a local event affecting the VS.

587 8. Tectonic model for the origin and evolution of the VS

588 8.1. Breakup

589 The JMFZ is usually interpreted as a consequence of plate tectonics
 590 involving the spreading between Eurasia and Greenland since Early
 591 Tertiary time (Talwani and Eldholm, 1977). However, the causes of
 592 segmentation of mid-oceanic ridges by long-lived transform boundaries
 593 such as the JMFZ are poorly understood. Even if the mechanisms leading to
 594 the initiation of the JMFZ remain unresolved due to unclear magnetic
 595 patterns masked by magmatism, we believe that the segmentation at the
 596 mature oceanic spreading stage may be directly linked to the latest
 597 continental rift configuration. The JMFZ seems to correlate with the crustal
 598 segmentation of the outer Vøring Basin and its transition zone toward the
 599 Møre margin (Gernigon et al., 2003). Berndt et al. (2001b) suggested a
 600 spatial correspondence of decreased volcanism and the location of the
 601 JMFZ influenced by the transform margin setting. Along margin

segmentation and the distribution of mafic intrusions at depth could
 602 most likely contribute to the localisation of the deformation and
 603 subsequent punctiform initiation of the spreading cells (e.g. Yamasaki
 604 and Gernigon, this volume). Most of previous studies have suggested that
 605 the location of the JMFZ was predisposed by the pre-breakup setting of the
 606 Mid-Norwegian margin. Doré et al. (1997) and Fichler et al. (1999)
 607 particularly note that the NW-SE lineaments, in the trend of the JMFZ, are
 608 sub-parallel to older, NW-SE Caledonian and/or Paleoproterozoic, deep-
 609 seated shear zones. They conclude that the Jan Mayen Lineament and the
 610 nascent JMFZ might have even been influenced by much older inherited
 611 structures. Other studies have also demonstrated that the pre-breakup
 612 segmentation has likely contributed to the location of similar, long-lived,
 613 oceanic transforms (Bonatti, 1996; Behn and Lin, 2000). 614

615 8.2. Post-breakup

After breakup, the JMFZ behaved as an oceanic transform (sensu
 616 stricto) and acted as a first-order discontinuity of the Norwegian-
 617 Greenland Sea, accommodating the sea-floor spreading at the Aegir and
 618 Mohns Ridges. The existence of a thick oceanic crust (> 15 km) below the
 619 VS provides evidence that large and anomalous melt production 620

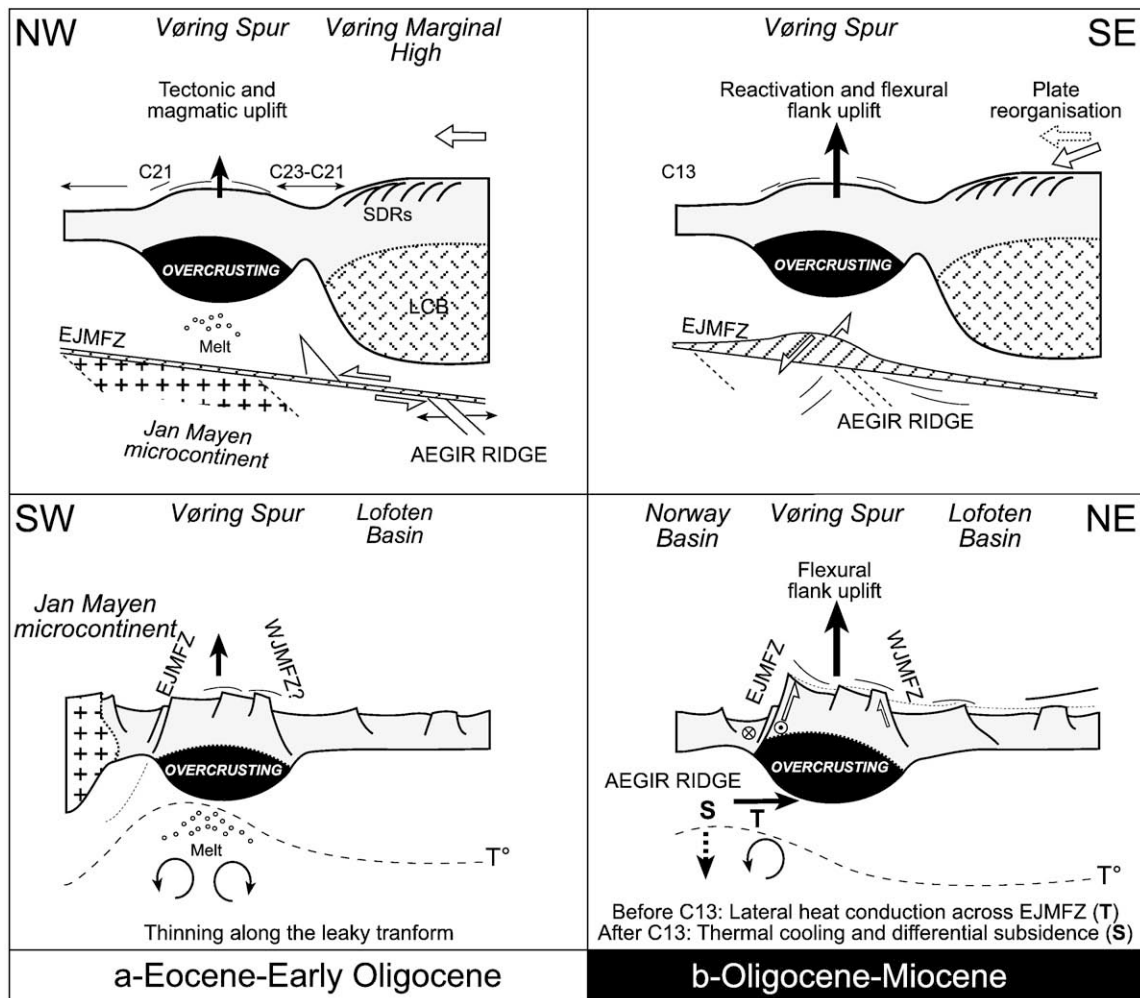


Fig. 14. Schematic cartoon summarising the magmato-tectonic and uplift evolution of the VS. a) Anomalous melt production generated during the oceanic accretion of the VS in Eocene time. A thin-spot and mantle upwelling along the JMFZ is proposed to explain the anomalous melt production on the VS. b) In our model, the VS is affected later by a flexural flank uplift driven by far-field normal stress and major faults reactivation. Heat transfer and differential thermal subsidence after abortion of the Aegir Ridge could also have affected the VS. LCB: lower crustal body, interpreted as mafic underplating emplaced during the breakup. SDRs: seaward-dipping reflectors emplaced along the continent-ocean transition.

persisted after the breakup of the Mid-Norwegian volcanic margin. The thickness of the crust is relatively similar in magnitude to that of the lower crustal body interpreted along the Vøring Marginal High. There, the thick high-velocity lower crust is linked with thick subaerial lava piles typically expressed as volcanic SDRs emplaced along the continent-ocean transition (Berndt et al., 2001a; Mjelde et al., 2007).

The present structure of the VS is the result of an intricate and long-lived period of block faulting and vertical tectonics initiated in Eocene time and active through the Oligocene and Miocene (Fig. 3). In our model, we propose that an overcrusting could have been produced along the trend of the JMFZ leading to the formation of an original thick oceanic crust in Mid- to Late Eocene time (Figs. 3, 14). Our hypothesis emerges as a viable alternative to the Late Miocene underplating hypothesis proposed by Breivik et al. (2008). Breivik et al. (2008) agree that the magmatism of the VS does not form a time-transgressive track, and does not fit a classic mantle plume model since magmatism occurs where the asthenospheric flow from the Iceland plume should normally have encountered a thicker lithosphere, not a thin-spot. Evidences of relatively thin and normal oceanic crust deduced from gravity inversion on either side of the JMFZ also does not favour the influence of an underlying plume either (Greenhalgh and Kusznir, 2007). To explain the atypical melt production of the VS, Breivik et al. (2008) suggested that partially molten mantle from the lowest part of the melt column was produced underneath the Aegir Ridge and captured by the asthenospheric flow from Iceland, before surfacing northeast of the EJMFZ. This model requires that the asthenosphere

can retain such a molten component over a significant time interval (10–15 Ma), but the reason for such a temporal delay in extracting the molten component remains unclear.

Although we do not reject this model, we call attention to the fact that most of the sedimentary sequences observed on seismic sections (Figs. 10, 11) are not really affected by significant intrusions and moreover there are no age dates to support any evidence for a major Late Miocene magmatic event near the VS. A seamant, located slightly before C5 (Early to Mid-Miocene), has been identified by Breivik et al. (2008) in the Norwegian-Greenland Sea, but farther to the north (~300 km). Breivik et al. (2008) claim that the basement-sediment interface could have acted as a density trap for heavy Late Miocene magma and consequently, the low density of the sediments could not facilitate the emplacement of sill intrusions. However, this argument is disputable and we believe that the major crustal fault zones in the close vicinity of the VS (Figs. 10, 11) would, on the contrary, have facilitated the upward migration of melts to the surface, as observed on the adjacent volcanic margin.

9. Discussion

9.1. Plate control on magmatism: observations and models at the scale of the Norwegian-Greenland Sea

Based on our new interpretation, we propose that the VS was a volcanic edifice formed during Mid- to Late Eocene time (Fig. 14a). We

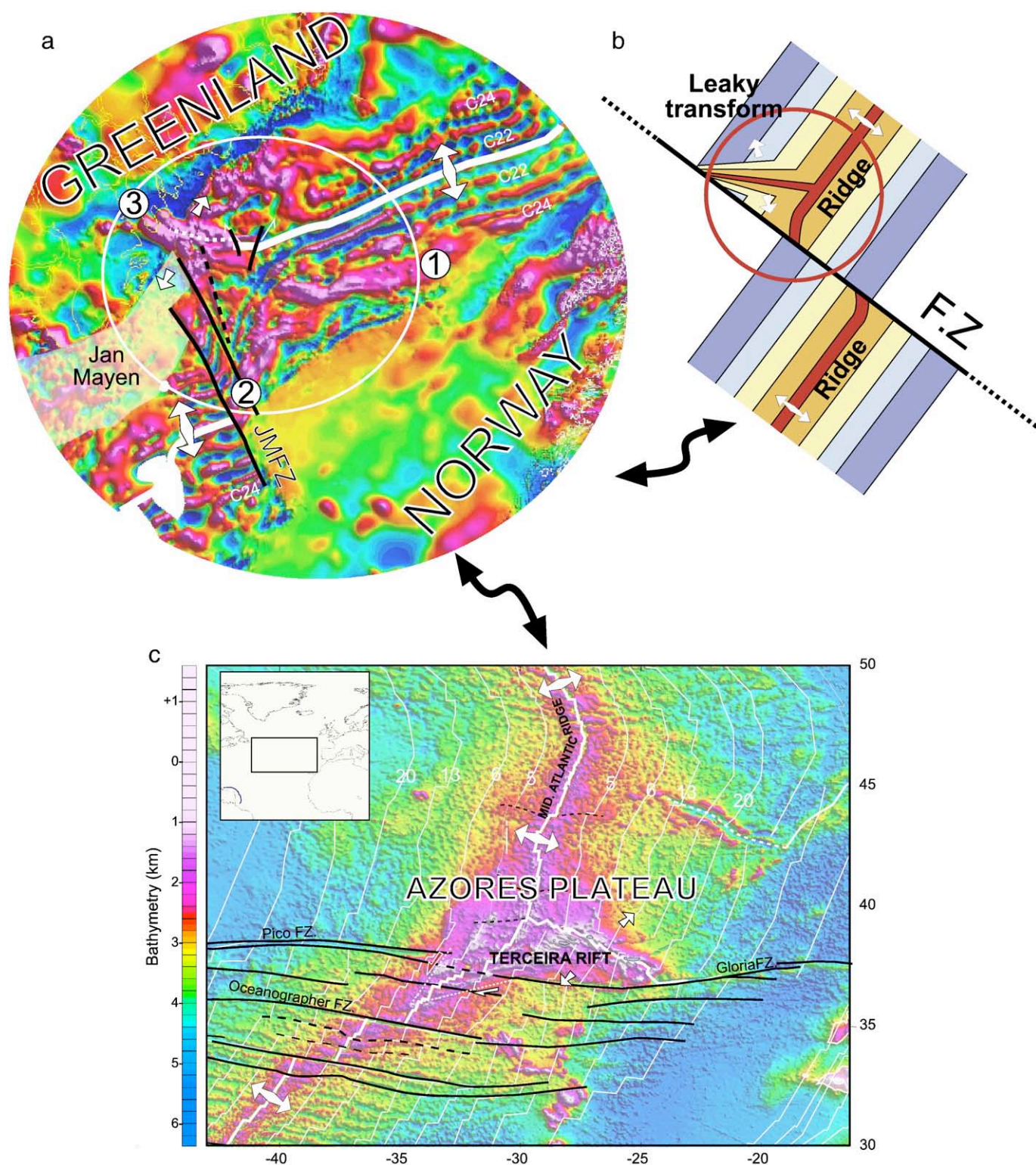


Fig. 15. a) Plate reconstruction of the Norwegian margin, Greenland and the Jan Mayen microcontinent, at C21 (~47 Ma ago). This picture illustrates a triple junction between two magnetic (magmatic) branches 1) and 2) which represent the basaltic SDRs along Vøring Marginal High and the Greenlandic part of the Traill-Vøring igneous complex (branch 3). In this kinematic reconstruction, the VS lies in the central part of the complex. Euler and rotation poles used for the reconstruction are described in Gaina et al. (2002). b) A leaky transform model can be proposed for both and the Traill-Vøring igneous complex lying in the trend of the VS could have formed obliquely along the trend of the pre-existing EJMfz. c) The Azores Plateau can be used as a modern analogue to the Jan Mayen spreading system, initiated 55 Ma ago. In the Azores Plateau, the situation is quite similar, a triple junction and volcanic traps formed along the spreading ridge and seem also to be influenced by the pre-existing oceanic fracture zones. A third branch (the Terceira Rift) propagates in transtension or/and as a slow rift from the spreading ridge toward the adjacent oceanic fracture zones (e.g. Gloria Fracture Zone). Isochrons from Müller et al. (1997).

668 suggest a genetic plate control of the JMFZ on the melt production and
 669 distribution since breakup time. Our observations of the VS area support
 670 an original idea proposed by Torske and Prestvik (1991) who considered

that the JMFZ represents a major lithospheric feature controlling the
 671 distribution and episodic and long-live formation of atypical magma-
 672 tism. Also, note that magmatism is still anomalous along the trend of the
 673

JMFZ as attested by the presence of the only Norwegian active stratovolcano (Beerenberg) on Jan Mayen (Fig. 1). Onshore Greenland, the Traill Ø basin is well-known for being intruded by a large number of igneous bodies, Eocene–Oligocene in age, concentrating along the trend of the JMFZ (Torske and Prestvik, 1991; Lundin and Doré, 2002; Olesen et al., 2007; Price et al., 1997). Based on wide-angle data, Schlindwein and Jokat (1997) stressed that this area also represents an important transfer zone between different crustal and basin architectures between Jameson Land and Traill Ø, in East Greenland. Offshore Traill Ø, a prominent E–W magnetic anomaly (Fig. 15) has been observed up to C21 (47 Ma) and interpreted as an igneous complex (the Traill–Vøring igneous complex) initiated during the early spreading history of the Norwegian–Greenland Sea (Olesen et al., 2007). In Eocene time, plate reconstruction (Fig. 15) suggests that the VS was situated between the Vøring Marginal High and the Traill–Vøring igneous complex, and we suggest that the VS was part of this larger magmatic complex.

A deep mantle plume and high temperatures are often invoked as the first-order parameter that controlled atypical melt production in oceanic domain (McKenzie and Bickle, 1988). Being aware that the plume and/or non-plume influence in the north Atlantic is a controversial issue (see Meyer et al., 2007 for a recent synthesis), we do not reject the idea that other dynamic or composition factors may have enhanced the melt production of the VS. The Greenland–Iceland–Faroës Ridge, initiated since the time of breakup, is surprisingly parallel to the JMFZ and also represents an excessive example of anomalously thick oceanic crust. The crust along the Greenland–Iceland–Faroës Ridge locally reaches a thickness of 38 to 40 km and is usually attributed to an elevated temperature (Smallwood et al., 1999). Nevertheless, some authors have claimed that the Greenland–Iceland–Faroës Ridge is simply the result of decompression of ‘cold’ melt-prone mantle materials influenced by the imprint of old Caledonian structures (Foulger et al., 2005). To some extent, but with large uncertainties, a similar setting cannot be totally excluded along the JMFZ and mantle rocks of ‘normal’ pyrolytic composition could eventually run both sub-parallel and transversely to the actual trend of the JMFZ. Local upwelling of melt-prone mantle material could be a possible model to explain part of the anomalous magmatic production observed along the trend of the JMFZ (e.g. Korenaga, 2004).

Independently of any fertile materials, plate processes alone can also explain the higher melt production along the JMFZ. Complex lithospheric stresses along the JMFZ can explain the long-lived magmatic activity and the increasing amount of melt observed along the fault zone. Previous contributions have shown that plate boundaries such as transform faults could channel magma to the surface and that there is a prevalence of ‘coincidental’ relationships between supposed hotspot features and pre-existing weakness zones (Beutel, 2005).

We propose that the JMFZ behaved as a leaky transform and may have been a kind of lithospheric thin-spot during the oceanic spreading and not necessarily a lithospheric barrier (Fig. 14a). Huang et al. (2003) provided numerical evidence that small-scale convection can develop beneath the transform itself. In their model, small-scale convection and increase of temperature can develop first below the pre-existing fracture zone with subsequent downwelling on the older side of the lithosphere across a fracture zone. Behn et al. (2007) have also shown that a rheology that incorporates brittle weakening of the lithosphere along the fracture zone can explain regions of enhanced mantle upwelling and elevated temperatures underneath a transform. Brittle weakening of the lithosphere and development of the leaky transform could explain enhanced mantle upwelling along the JMFZ. This could have enhanced mantle decompression and partial melting along the VS compared to surrounding oceanic domains (Fig. 14a).

9.2. The Eocene Norwegian spreading system: why not a triple junction?

Plate reconstructions of the early spreading configuration in the Norwegian–Greenland Sea, suggest a connection between the Vøring

Marginal High, the VS and the Traill–Vøring Igneous Complex, offshore Greenland (Fig. 15a). Restored at Eocene time, the proposed kinematic fit of the magnetic anomalies highlights three prominent magnetic (and magmatic) anomalies, which meet at near 120° angles (Fig. 15a). We propose that the Traill–Vøring igneous complex and VS, located in the central part of the triple junction, were genetically associated with the Vøring Marginal High convex volcanic rift system in a kind of triple junction during the early stage of oceanic spreading.

In this model, the distribution of the anomalous magmatism, observed at the VS level, is explained by a discrete leaky transform (or oblique crack) developing along the JMFZ. Regional NW–SE to E–W spreading along the Norwegian–Greenland Sea could have been locally perturbed near the pre-existing JMFZ, leading to transtension and formation of the leaky transform, similar to the scheme proposed by Searle (1980) to describe the formation of a triple junction (Fig. 15b). Similar “cracks arms” propagating from banded volcanic rifts could have been enhanced by self-induced stress as described by McHone et al. (2005).

Oblique normal stresses at the ridge–transform intersection may have caused normal faulting and lithospheric thinning in an orientation incompatible with the Aegir Ridge propagation. Lithospheric weakening and thinning may have subsequently resulted in a local upwelling and decompression melting of the upper mantle underneath the VS. The three spreading/transform branches probably formed a triple junction where anomalous melt production was initiated along the Vøring Marginal High during the breakup, and continued episodically to the west along the trend of the JMFZ. Melt production developed preferentially near the oceanic transform, which also created a major pathway for magma to reach the surface.

An analogue scenario can be observed along the active and more exotic Azores system (Fig. 15c). The Azores Plateau is a first-order morphological and magmatic feature in the Atlantic and the tectono-magmatic setting is relatively similar (Cannat et al., 1999; Luis and Miranda, submitted for publication; Searle, 1980). In the Azores, a triple junction that initiated about 30 Ma ago along the main spreading system was affected by pre-existing oceanic fracture zones (e.g. Pico and Gloria Fracture Zones) (Fig. 15c). For comparison, structures like the VS or the Traill–Vøring igneous complex could have behaved, at some stage, as a leaky transform axis, quite similar to the Terceira “Rift” described in the Azores Plateau (Searle, 1980; Vogt and Jung, 2004). This morphological high was formed during the past twenty million years by tectonic and volcanic processes resulting from the interaction of three major plates (Lourenco et al., 1998; Luis and Miranda, submitted for publication).

Although the Azores swell has a well-developed topographic and gravity signature, like the VS, its origin is still uncertain (Luis and Neves, 2006) and a mantle plume influence is still debatable (Bonatti, 1990; Cannat et al., 1999). The Azores Plateau is also supported by a thickened crust, which mainly results from large volumes of accreted extrusives rocks and consequent deflection of the underlying elastic plate (Luis and Neves, 2006). Both the free air gravity and the mantle Bouguer admittance point to a flexural isostatic model with a Moho depth of 12 km and an elastic thickness in the range of 3–6 km (Luis and Neves, 2006). A thick oceanic crust in the Azores was also suggested by an earlier Rayleigh-wave dispersion study, which indicated that the upper mantle seismic velocities beneath the Azores Plateau are anomalously low (Searle, 1976). Even if more work needs to be carried out in the future to validate such an hypothesis, the analogy between the Azores and the Jan Mayen system is attractive and a similar triple junction model could be proposed here as a challenging working hypothesis to explain the large volumes of magma produced along the Vøring Marginal High and the trend of the JMFZ.

10. Summary

In this paper, we have investigated the structure and tectono-magmatic processes operating along the JMFZ during and after continental breakup. We have presented the new results of the JAS-05 aeromagnetic

survey and its interpretation. The new magnetic grid allowed us to better identify magnetic chrons and faults zones, leading to an update of the geophysical and tectonic background of the early spreading system in the vicinity of the JMFZ.

This study has focused on the VS, an anomalous oceanic high lying north of the EJMFZ. We have showed that the structure and the low Bouguer gravity signature of the VS can be explained by the atypical thickness of the oceanic crust below the VS, which locally reach 15 km. We propose that this thick oceanic crust, so-called overcrusting, was syn-accretion and formed during Mid- to Late Eocene time.

A change of spreading direction could have increased the normal stress along the EJMFZ leading to a subsequent and progressive, flexural flank uplift of the VS. Buoyancy forces due to the overcrusting, a lateral temperature gradient and later differential subsidence on either side of the EJMFZ are expected to have influenced the final geometry of the VS.

The large melt production initiated along the Vøring Marginal High during the breakup continued episodically along the trend of the JMFZ. The local increase of magma production along the JMFZ suggests that the oceanic transform acted, and still acts, as a long-lived magmatic pathway for melts in the lithosphere. During the spreading of the Norwegian–Greenland Sea, lithospheric weakening, thin-spot, mantle upwelling and decompression are expected to have occurred along the JMFZ and locally could have facilitated on increased melt production compared to the situation in the Norway and Lofoten Basins.

Plate reconstruction suggests that a triple junction, similar to the Azores Plateau system, could have been initiated slightly after the breakup between the Vøring Marginal High, the VS and the Traill–Vøring igneous complex, now located offshore Greenland. Volcanic activity may have increased locally along a leaky transform acting as the third branch of the junction, slightly oblique to the pre-existing EJMFZ. The new data confirm that most of the fundamental structures of the oceanic basins of the Norwegian Sea and adjacent margins are more complex than previously thought. The present paper illustrates the importance of the oceanic fracture zones in lithospheric upwelling, active mantle decompression, and melt production. They might provide clues to help understand the evolution of further oceanic controversial features, such as the Greenland–Faroes–Iceland Ridge, or simply to better understand the processes involved during the breakup of the Mid-Norwegian volcanic margin. Nevertheless, more work needs to be carried out and future data acquisition is definitively required to solve the complex magmato-tectonic puzzle of the Norwegian–Greenland Sea.

Acknowledgements

The present paper summarises part of the results obtained at NGU during the JAS-05 project co-funded by NGU, NPD, Shell and StatoilHydro. Jaap Mondt, Olav Norvik (Shell) and Øyvind Steen (StatoilHydro) provided advice during the JAS-05 acquisition. NPD kindly provided seismic, high-resolution bathymetric and other aeromagnetic data from the Jan Mayen–Vøring area. TGS allowed us to use the VBE-AM-00 survey acquired along the Vøring Transform. The grid rotation program, developed by M. Smethurst, was used for the plate reconstruction of the VS. The 2.5D gravity modelling was carried out using an Interactive Gravity and Magnetic Application System (IGMAS; <http://www.gravity.uni-kiel.de/igmas>). The magnetic anomalies have been modelled using the Modmag Matlab program developed by V. Mendel, M. Muncshy and D. Sauter at Institut de Physique du Globe de Strasbourg. We thank J. Skogseid and M. Cannat for their constructive and fair reviews which significantly improved the original manuscript. We are also indebted to S. McEnroe and D. Roberts for improving the English in the final manuscript. We thank all these persons, companies and institutions.

References

Andersen, O.B., Knudsen, P., 1998. Gravity Anomalies Derived from the ERS-1 Satellite Altimetry. Kort og Matrikelstyrelsen, DK-2400 Copenhagen NV, Denmark. (www.kms.dk).

- Baines, A.G., Cheadle, M.J., Dick, H.J.B., Scheirer, A.H., John, B.E., Kuszniir, N.J., Matsumoto, T., 2003. Mechanism for generating the anomalous uplift of oceanic core complexes: Atlantis Bank, southwest Indian Ridge. *Geology* 31 (12), 1105–1108. 866
- Behn, M.D., Boettcher, M.S., Hirth, G., 2007. Thermal structure of oceanic transform faults. *Geology* 35 (4), 307–310. 868
- Behn, M.D., Lin, J., 2000. Segmentation in gravity and magnetic anomalies along the US East Coast passive margin: implications for incipient structure of the oceanic lithosphere. *Journal of Geophysical Research—Solid Earth* 105 (B11), 25769–25790. 870
- Berndt, C., Planke, S., Alvestad, E., Tsikalas, F., Rasmussen, T., 2001a. Seismic volcanostratigraphy of the Norwegian Margin: constraints on tectonomagmatic break-up processes. *Journal of the Geological Society* 158, 413–426. 874
- Berndt, C., Mjelde, R., Planke, S., Shimamura, H., Faleide, J.I., 2001b. Controls on the tectono-magmatic evolution of a volcanic transform margin: the Vøring Transform Margin, NE Atlantic. *Marine Geophysical Researches* 22 (3), 133–152. 877
- Beutel, E.K., 2005. Stress-induced seamount formation at ridge–transform intersections. In: Foulger, G.R., Natland, J.H., Presnall, D.C., Anderson, D.L. (Eds.), *Plates, Plumes and Paradigms*. Geological Society of America Special Paper, vol. 338, pp. 581–593. 880
- Blystad, P., Brekke, H., Færseth, R.B., Larsen, B.T., Skogseid, J., Tørudbakken, B., 1995. Structural elements of the Norwegian continental shelf, Part II. The Norwegian Sea Region. *Norwegian Petroleum Directorate Bulletin*, vol. 8, pp. 0–45. 883
- Bonatti, E., 1990. No so hot “hot-spots” in the oceanic mantle. *Science* 250 (4977), 107–111. 885
- Bonatti, E., 1996. Anomalous opening of the Equatorial Atlantic due to an equatorial mantle thermal minimum. *Earth and Planetary Science Letters* 143 (1–4), 147–160. 887
- Bonatti, E., Ligì, M., Gasperini, L., Peyve, A., Ranzitini, Y., Chen, Y.J., 1994. Transform migration and vertical tectonics at the Romanche fracture zone, Equatorial Atlantic. *Journal of Geophysical Research, B, Solid Earth and Planets* 99, 21,779–21,802. 890
- Breivik, A.J., Mjelde, R., Faleide, J.I., Murai, Y., 2006. Rates of continental breakup magmatism and seafloor spreading in the Norway Basin–Iceland plume interaction. *Journal of Geophysical Research—Solid Earth* 111 (B7), B07102. doi:10.1029/2005JB004004. 893
- Breivik, A., Faleide, J.I., Mjelde, R., 2008. Neogene magmatism northeast of the Aegir and Kolbeinsey ridges, NE Atlantic: spreading ridge mantle plume interaction? G-Cube. *Geochemistry Geophysics Geosystem an Electronic Journal of the Earth Sciences* 9 (2), Q02004. doi:10.1029/2007GC001750. 898
- Brekke, H., 2000. The tectonic evolution of the Norwegian Sea continental margin with emphasis on the Vøring and Møre basins. In: Nøttvedt, A., et al. (Ed.), *Dynamics of the Norwegian Margin*. Special Publications, vol. 136. Geological Society, London, pp. 327–378. 902
- Bugge, T., Eidvin, T., Smelror, M., Ayers, S., Ottesen, D., Rise, L., Andersen, E.S., Dahlgren, T., Evands, D., Henriksen, S., 2004. In: Martinsen, O. (Ed.), *Deep Water Sedimentary Systems of Arctic and North Atlantic Margins*. Geological Society of Norway, NGF Abstracts and Proceedings, vol. 1, pp. 14–15. 906
- Cande, S.C., Kent, D.V., 1995. Revised calibration of the geomagnetic polarity timescale for the Late Cretaceous and Cenozoic. *Journal of Geophysical Research* 100 (B4), 6093–6095. 909
- Cannat, M., Briais, A., Deplus, C., Escartin, J., Georgen, J., Lin, J., Mercouriev, S., Meyzen, C., Muller, M., Pouliquen, G., Rabain, A., da Silva, P., 1999. Mid-Atlantic Ridge–Azores hotspot interactions: along-axis migration of a hotspot-derived event of enhanced magmatism 10 to 3 Ma ago. *Earth and Planetary Science Letters* 173 (3), 257–269. 913
- Compagnie Générale de Géophysique. 1977. Norwegian Petroleum Directorate, Aeromagnetic Survey Jan Mayen Area, Interpretation Report. 23p (unpublished). 914
- Chen, Y., 1988. Thermal model of oceanic transform faults. *Journal of Geophysical Research* 93, 8839–8851. 917
- Cooper, G.R.J., Cowan, D.R., 2006. Enhancing potential field data using filters based on the local phase. *Computers & Geosciences* 32 (10), 1585–1591. 919
- Doré, A.G., Lundin, E.R., Fichler, C., Olesen, O., 1997. Patterns of basement structure and reactivation along the NE Atlantic margin. *Journal of the Geological Society* 154, 85–92. 921
- Eldholm, O., Grue, K., 1994. North-Atlantic volcanic margins – dimensions and production-rates. *Journal of Geophysical Research—Solid Earth* 99 (B2), 2955–2968. 923
- Faugères, J.C., Stow, D.A.V., Imbert, P., Viana, A., 1999. Seismic features diagnostic of contourite drifts. *Marine Geology* 162 (1), 1–38. 925
- Fichler, C., Rundhovde, E., Olesen, O., Sæther, B.M., Rueslåtten, H., Lundin, E., Doré, A.G., 1999. Regional tectonic interpretation of image enhanced gravity and magnetic data covering the mid-Norwegian shelf and adjacent mainland. *Tectonophysics* 306 (2), 183–197. 929
- Foulger, G.R., Natland, H., Anderson, L., 2005. A source for Icelandic magmas in remelted lapetus crust. *Journal of Volcanology and Geothermal Research* 141, 23–44. 931
- Gaina, C., Roest, W.R., Müller, R.D., 2002. Late Cretaceous–Cenozoic deformation of northeast Asia. *Earth and Planetary Science Letters* 197, 273–286. 933
- Geoffroy, L., 2005. Volcanic passive margins. *Comptes Rendus Geoscience* 337 (16), 934–935. 935
- Geosoft, 2005. *Montaj GridKnit, Grid extension for OASIS Montaj v. 6.1, Tutorial and User Guide*. Geosoft Incorporated. 27pp. 937
- Gernigon, L., Lucazeau, F., Brigaud, F., Ringenbach, J.C., Planke, S., Le Gall, B., 2006. A moderate melting model for the Vøring margin (Norway) based on structural observations and a thermo-kinematical modelling: implication for the meaning of the lower crustal bodies. *Tectonophysics* 412 (3–4), 255–278. 941
- Gernigon, L., Olesen, O., Koziel, J., and Lynum, R., 2008. Norway Basin aeromagnetic survey (NB-07) acquisition, processing, Geological Survey of Norway (NGU). Unpublished. 944
- Gernigon, L., Ringenbach, J.C., Planke, S., Le Gall, B., Jonquet-Kolstø, H., 2003. Extension, crustal structure and magmatism at the outer Vøring Basin, Norwegian margin. *Journal of the Geological Society* 160 (2), 197–208 (12). 946
- Goll, R.M., 1989. A synthesis of Norwegian Sea biostratigraphies: ODP Leg 104 on the Vøring Plateau. In: Eldholm, O., Thiede, J., Taylor, B., et al. (Eds.), *Proceedings of the* 949

- Ocean Drilling Program, Scientific Results, vol. 104. Ocean Drilling Program, College Station, TX, pp. 777–826.
- Greenhalgh, E.E., Kusznir, N.J., 2007. Evidence for thin oceanic crust on the extinct Aegir Ridge, Norwegian Basin, NE Atlantic derived from satellite gravity inversion. *Geophysical Research Letters* 34 (6), L06305. doi:10.1029/2007GL029440.
- Gudlaugsson, S.T., Gunnarsson, K., Sand, M., Skogseid, J., 1988. Tectonic and volcanic events at the Jan Mayen Ridge microcontinent. In: Morton, A.C., Parson, L.M. (Eds.), *Early Tertiary Volcanism and the Opening of the NE Atlantic*. Special Publications, vol. 39. Geological Society, pp. 85–86.
- Hagevang, T., Eldholm, O., Aalstad, I., 1983. Pre-23 magnetic anomalies between Jan Mayen and Greenland–Senja Fracture Zones in the Norwegian Sea. *Marine Geophysical Researches* 5, 345–363.
- Henriksen, S., Vorren, T.O., 1996. Late Cenozoic sedimentation and uplift history on the mid-Norwegian continental shelf; impact of glaciations on basin evolution; data and models from the Norwegian margin and adjacent areas. *Global and Planetary Change* 12, 171–199.
- Hjelstuen, B.O., Eldholm, O., Faleide, J.I., 2007. Recurrent Pleistocene mega-failures on the SW Barents Sea margin. *Earth and Planetary Science Letters* 258 (3–4), 605–618.
- Huang, J., Zhong, S., van Hunen, J., 2003. Controls on sublithospheric small-scale convection. *Journal of Geophysical Research*, 108 (B8, 2405). doi:10.1029/2003JB002456.
- Johnson, G.L., Eckhoff, O.B., 1966. Bathymetry of the north Greenland Sea. *Deep Sea Research* 13, 1161–1173.
- Jung, W.Y., Vogt, P.R., 1997. A gravity and magnetic anomaly study of the extinct Aegir Ridge, Norwegian Sea. *Journal of Geophysical Research* 12 (B3), 5065–5089.
- Korenaga, J., 2004. Mantle mixing and continental breakup magmatism. *Earth and Planetary Science Letters* 218 (3–4), 463–473.
- Kusznir, N.J., Karner, G.D., 2007. Continental lithospheric thinning and breakup in response to upwelling divergent mantle flow: application to the Woodlark, Newfoundland and Iberia margins. *Geological Society, London, Special Publications* 282 (1), 389–419.
- Laberg, J.S., Dahlgren, T., Vorren, T.O., Hafliðason, H., Bryn, P., 2001. Seismic analyses of Cenozoic contourite drift development in the Northern Norwegian Sea. *Marine Geophysical Researches* 22 (5–6), 401–416.
- Laxon, S., McAdoo, D., 1994. Arctic-ocean gravity-field derived from ERS-1 satellite altimetry. *Science* 265 (5172), 621–624.
- Lien, T., 2005. From rifting to drifting: effects on the development of deep-water hydrocarbon reservoirs in a passive margin setting, Norwegian Sea. *Norwegian Journal of Geology* 85 (4), 319–332.
- Lourenco, N., Miranda, J.M., Luis, J.F., Ribeiro, A., Victor, L.A.M., Madeira, J., Needham, H.D., 1998. Morpho-tectonic analysis of the Azores Volcanic Plateau from a new bathymetric compilation of the area. *Marine Geophysical Researches* 20 (3), 141–156.
- Lucazeau, F., Brigaud, F., Leturmy, P., 2003. Dynamic interactions between the Gulf of Guinea passive margin and the Congo River drainage basin: 2. Isostasy and uplift. *Journal of Geophysical Research—Solid Earth* 108 (B8). doi:10.1029/2002JB001928.
- Luis, J.F. and Miranda, J.M., submitted for publication. Re-evaluation of magnetic chrons in the North-Atlantic between 35 N and 55 N: implication for the onset of the Azores. *Journal of Geophysical Research*.
- Luis, J.F., Neves, M.C., 2006. The isostatic compensation of the Azores Plateau: a 3D admittance and coherence analysis. *Journal of Volcanology and Geothermal Research* 156 (1–2), 10–22.
- Lundin, E., Doré, A.G., 2002. Mid-Cenozoic post-breakup deformation in the 'passive' margins bordering the Norwegian–Greenland Sea. *Marine and Petroleum Geology* 19 (1), 79–93.
- Luyendyk, A.P.J., 1997. Processing of airborne magnetic data. *AGSO Journal of Australian Geology and Geophysics* 17 (2), 31–38.
- Mauring, E., Beard, L.P., Kihle, O., Smethurst, M.A., 2002. A comparison of aeromagnetic levelling techniques with an introduction to median levelling. *Geophysical Prospecting* 50 (1), 43–54.
- McHone, J.G., Anderson, D.L., Beutel, E.K., Fialko, Y.A., 2005. Giant dikes, rifts, flood basalts and plate tectonics: a contention of mantle models. In: Foulger, G.R., Natland, J.H., Presnall, D.C., Anderson, D.L. (Eds.), *Plates, Plumes and Paradigms*. Geological Society of America Special Paper, pp. 401–420.
- McKenzie, D.P., Bickle, M.J., 1988. The volume and composition of melt generated by extension of the lithosphere. *Journal of Petrology* 29, 625–679.
- Meyer, R., van Wijk, J.W., Gernigon, L., 2007. An integrated geophysical and geochemical model for North Atlantic Igneous Province magmatism. In: Foulger, G.R., Jurdy, D.M. (Eds.), *Plates, Plumes, and Planetary Processes*. Geological Society of America Special Paper, vol. 430, pp. 525–552.
- Mjelde, R., Raum, T., Murai, Y., Takanami, T., 2007. Continent–ocean-transitions: review, and a new tectono-magmatic model of the Voring Plateau, NE Atlantic. *Journal of Geodynamics* 43 (3), 374–392.
- Mosar, J., Eide, E.A., Osmundsen, P.T., Sommaruga, A., Torsvik, T.H., 2002. Greenland–Norway separation: a geodynamic model for the North Atlantic. *Norwegian Journal of Geology* 82 (4), 281–298.
- Myhre, A., Eldholm, A., 1980. Sedimentary and crustal velocities in the Norwegian–Greenland Sea. *Journal of Geophysical Research* 86 (B6), 5012–5022.
- Müller, R.D., Roest, W.R., Royer, J.Y., Gahagan, L.M., Sclater, J.G., 1997. Digital isochrons of the world's ocean floor. *Journal of Geophysical Research—Solid Earth* 102 (B2), 3211–3214.
- Nunns, A.G., 1982. The structure and evolution of the Jan Mayen Ridge and surroundings regions. *Memoirs of the American Association of Petroleum Geologists* 34, 193–208.
- Olesen, O., Gellein, J., Håbrekke, H., Kihle, O., Skilbrei, J.R., Smethurst, M., 1997a. Magnetic anomaly map Norway and adjacent ocean areas, scale 1:3 million. Norges geologiske undersøkelse (NGU). Trondheim, Norway.
- Olesen, O., Torsvik, T.H., Tveten, E., Zwaan, K.B., Løseth, H., Henningsen, T., 1997b. 1035
Basement structure of the continental margin in the Lofoten–Lopphavet area, 1036
northern Norway: constraints from potential field data, on-land structural mapping 1037
and palaeomagnetic data. *Norsk Geologisk Tidsskrift* 77 (1), 15–30. 1038
- Olesen, O., Gernigon, L., Ebbing, J., Mogaard, J.O., Pascal, C., Wienecke, S., 2006. 1039
Interpretation of Aeromagnetic Data along the Jan Mayen Fracture Zone, JAS-05, 1040
Geological Survey of Norway (NGU). Trondheim. Report 2006.018. 162 pp. 1041
- Olesen, O., Ebbing, J., Lundin, E., Mauring, E., Skilbrei, J.R., Torsvik, T.H., Hansen, E.K., 1042
Henningsen, T., Midboe, P., Sand, M., 2007. An improved tectonic model for the 1043
Eocene opening of the Norwegian–Greenland Sea: use of modern magnetic data. 1044
Marine and Petroleum Geology 24 (1), 53–66. 1045
- Osmundsen, P.T. and Ebbing, J., Submitted for publication. Styles of extension offshore 1046
Mid-Norway and implications for mechanisms of Late Jurassic–Early Cretaceous. 1047
Tectonics. 1048
- Parsons, B., Sclater, J.G., 1977. An analysis of the variation of ocean floor bathymetry and 1049
heat flow with age. *Journal of Geophysical Research* 82, 803–827. 1050
- Praeg, D., Stoker, M.S., Shannon, P.M., Ceramicola, S., Hjelstuen, B., Laberg, J.S., 1051
Mathiesen, A., 2005. Episodic Cenozoic tectonism and the development of the 1052
NW European 'passive' continental margin. *Marine and Petroleum Geology* 22 (9– 1053
10), 1007–1030. 1054
- Price, S.P., Brodie, J.A., Whitham, A.G., Kent, R., 1997. Mid-Tertiary rifting and 1055
magmatism in the Traill Ø region, East Greenland. *Journal of the Geological Society* 1056
London 154, 419–434. 1057
- Ren, S.C., Skogseid, J., Eldholm, O., 1998. Late Cretaceous–Paleocene extension on the 1058
Voring Volcanic Margin. *Marine Geophysical Researches* 20 (4), 343–369. 1059
- Sandwell, D.T., Smith, W.H.F., 1997. Marine gravity anomaly from Geosat and ERS1 1060
satellite altimetry. *Journal of Geophysical Research* 102 (B5), 10039–10054. 1061
- Scheck-Wenderoth, M., Raum, T., Faleide, J.I., Mjelde, R., Horsfield, B., 2007. The 1062
transition from the continent to the ocean: a deeper view on the Norwegian 1063
margin. *Journal of the Geological Society, London* 164, 8555–8868. 1064
- Schindwein, V., Jokat, W., 1997. Structure and evolution of the continental crust of 1065
northern east Greenland from integrated geophysical studies. *Journal of Geophysical* 1066
Research 104 (B7), 15227–15245. 1067
- Scott, R.A., Ramsey, L.A., Jones, S.M., Sinclair, S., Pickles, C.S., 2005. Development of the Jan 1068
Mayen microcontinent by linked propagation and retreat of spreading ridges. In: 1069
Wandås, B.T.G., J.P. Nystuen, E., Eide, Gradstein, F. (Eds.), *Onshore–Offshore Relations* 1070
on the North Atlantic Margin. Norwegian Petroleum Society, pp. 69–82. 1071
- Searle, R., 1976. Lithospheric structure of the Azores Plateau from Rayleigh-wave 1072
dispersion. *Geophysical Journal of the Royal Astronomical Society* 44, 537–546. 1073
- Searle, R.C., 1980. Tectonic pattern of the Azores spreading centre and triple junction. 1074
Earth and Planetary Science Letters 51, 415–434. 1075
- Skilbrei, J.R., Olesen, O., Osmundsen, P.T., Kihle, O., Aaro, S., Fjellanger, E., 2002. A study 1076
of basement structures and onshore–offshore correlations in Central Norway. 1077
Norwegian Journal of Geology 82 (4), 263–279. 1078
- Skogseid, J., Eldholm, O., 1987. Early Cenozoic crust at the Norwegian Continental- 1079
Margin and the conjugate Jan-Mayen Ridge. *Journal of Geophysical Research—Solid* 1080
Earth and Planets 92 (B11), 11471–11491. 1081
- Skogseid, J., Pedersen, T., Eldholm, O., Larsen, B.T., 1992. Tectonism and magmatism 1082
during NE Atlantic continental break-up: the Voring basin. In: Storey, B.C., 1083
Alabaster, T., Plankhurst, R.J. (Eds.), *Magmatism and the Causes of Continental* 1084
Break-up. Special Publications. Geological Society, London, pp. 305–320. 1085
- Smallwood, J.R., Staples, R.K., Richardson, K.R., White, R.S., 1999. Crust generated above 1086
the Iceland mantle plume: from continental rift to oceanic spreading center. *Journal* 1087
of Geophysical Research—Solid Earth 104 (B10), 22885–22902. 1088
- Sirastava, S., Tapscott, C.R., 1986. Plate kinematics of the North Atlantic. In: Vogt, P.R., 1089
Tucholke, B.E. (Eds.), *The Geology of North America, Volume M, The Western North* 1090
Atlantic Region. Geological Society of America, pp. 379–404. 1091
- Stoker, M.S., Praeg, D., Hjelstuen, B.O., Laberg, J.S., Nielsen, T., Shannon, P.M., 2005. 1092
Neogene stratigraphy and the sedimentary and oceanographic development of the 1093
NW European Atlantic margin. *Marine and Petroleum Geology* 22 (9–10), 1094
977–1005. 1095
- Stuevold, L.M., Eldholm, O., 1996. Cenozoic uplift of Fennoscandia inferred from a study 1096
of the mid-Norwegian margin. *Global and Planetary Change* 12 (1–4), 359–386. 1097
- Symonds, P.A., Brekke, H., 2004. The ridge provisions of Article 76 of UN Convention on 1098
the Law of the Sea. In: Nordquist, M.H., Norton Moore, J., Heidar, T.H. (Eds.), *Legal* 1099
and Scientific Aspects of Continental Shelf Limits. Martinus Nijhoff Publishers, 1100
Laiden, pp. 169–199. 1101
- Talwani, M., Eldholm, O., 1977. Evolution of the Norwegian–Greenland Sea. *Geological* 1102
Society of America Bulletin 88 (7), 969–999. 1103
- TGS-NOPEC Geophysical Company, 2000. High-density Aeromagnetic Survey VBEAM- 1104
00 at Outer Voring Basin, Norwegian Sea, Processing Report. Commercial report, 1105
unpublished, TGS-NOPEC. 1106
- Torske, T., Prestvik, T., 1991. Mesozoic detachment faulting between Greenland and 1107
Norway: inferences from Jan Mayen Fracture Zone system and associated alkalic 1108
volcanic rocks. *Geology* 19, 481–484. 1109
- Torsvik, T.H., Mosar, J., Eide, E., 2001. Cretaceous–Tertiary geodynamics: a North Atlantic 1110
exercise. *Geophysical Journal International* 146, 850–866. 1111
- Tsikalas, F., Eldholm, O., Faleide, J.I., 2002. Early Eocene sea floor spreading and 1112
continent–ocean boundary between Jan Mayen and Senja fracture zones in the 1113
Norwegian–Greenland Sea. *Marine Geophysical Researches* 23 (3), 247–270. 1114
- Untemehr, P., 1982. Etude structurale et cinématique de la mer de Norvège et du Greenland- 1115
Evolution du microcontinent de Jan Mayen. Université de Brest, Brest 0–227 pp. 1116
Q10
- van Wijk, J.W., Huismans, R.S., ter Voorde, M., Cloetingh, S., 2001. Melt generation at 1117
volcanic continental margins: no need for a mantle plume? *Geophysical Research* 1118
Letters 28 (20), 3995–3998. 1119

- 1120 Verhoef, J., Roest, W.R., Macnab, R., Arkani-Hamed, J., Members of the Project Team, 1121
1122 1997. Magnetic Anomalies of the Arctic and North Atlantic Oceans and Adjacent
1123 Land Areas. *Journal of Geophysical Research* 102, 11245–11254.
- 1123 Vogt, P.R., Jung, W.Y., 2004. The Terceira Rift as hyper-slow, hotspot-dominated oblique
1124 spreading axis: a comparison with other slow-spreading plate boundaries. *Earth
1125 and Planetary Science Letters* 218 (1–2), 77–90.
- 1126 Vogt, P.R., Taylor, P., Kovacs, L.C., Johnson, G.L., 1979. Detailed aeromagnetic investiga-
1127 tion of the Arctic Basin. *Journal of Geophysical Research* 84, 1071–1089.
- 1134
- Wessel, P., Haxby, W.F., 1990. Thermal stresses, differential subsidence, and flexure at 1128
oceanic fracture zones. *Journal of Geophysical Research* 95, 375–391. 1129
- Wienecke, S., Braitenberg, C., Götze, H.J., 2007. A new analytical solution estimating the 1130
flexural rigidity in the Central Andes. *Geophysical Journal International* 169, 1131
789–794. 1132
1133

UNCORRECTED PROOF